Modelling the continuum of macrophage phenotypes and their role in inflammation

Almansour, S., Dunster, J. L. ORCID: https://orcid.org/0000-0001-8986-4902, Crofts, J. J. and Nelson, M. ORCID: https://orcid.org/0000-0001-5320-2464 (2024) Modelling the continuum of macrophage phenotypes and their role in inflammation. Mathematical Biosciences, 377. 109289. ISSN 1879-3134 doi: https://doi.org/10.1016/j.mbs.2024.109289 Available at https://centaur.reading.ac.uk/118612/

Mathematical Biosciences 377 (2024) 109289

Contents lists available at ScienceDirect

Mathematical Biosciences

journal homepage: www.elsevier.com/locate/mbs

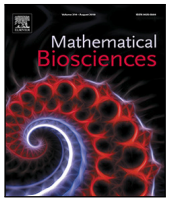

Original research article

Modelling the continuum of macrophage phenotypes and their role in inflammation

Suliman Almansour [a], Joanne L. Dunster [b], Jonathan J. Crofts [a], Martin R. Nelson [a,*]

[a] School of Science & Technology, Nottingham Trent University, Nottingham, NG11 8NS, UK
[b] Institute for Cardiovascular and Metabolic Research, University of Reading, Reading, RG6 6AS, UK

ARTICLE INFO

Keywords:
Macrophage
Inflammation
Bifurcation analysis
XPPAUT

ABSTRACT

Macrophages are a type of white blood cell that play a significant role in determining the inflammatory response associated with a wide range of medical conditions. They are highly plastic, having the capacity to adopt numerous polarisation states or 'phenotypes' with disparate pro- or anti-inflammatory roles. Many previous studies divide macrophages into two categorisations: M1 macrophages are largely pro-inflammatory in nature, while M2 macrophages are largely restorative. However, there is a growing body of evidence that the M1 and M2 classifications represent the extremes of a much broader spectrum of phenotypes, and that intermediate phenotypes can play important roles in the progression or treatment of many medical conditions. In this article, we present a model of macrophage dynamics that includes a continuous description of phenotype, and hence incorporates intermediate phenotype configurations. We describe macrophage phenotype switching via nonlinear convective flux terms that scale with background levels of generic pro- and anti-inflammatory mediators. Through numerical simulation and bifurcation analysis, we unravel the model's resulting dynamics, paying close attention to the system's multistability and the extent to which key macrophage–mediator interactions provide bifurcations that act as switches between chronic states and restoration of health. We show that interactions that promote M1-like phenotypes generally result in a greater array of stable chronic states, while interactions that promote M2-like phenotypes can promote restoration of health. Additionally, our model admits oscillatory solutions reminiscent of relapsing–remitting conditions, with macrophages being largely polarised toward anti-inflammatory activity during remission, but with intermediate phenotypes playing a role in inflammatory flare-ups. We conclude by reflecting on our observations in the context of the ongoing pursuance of novel therapeutic interventions.

1. Introduction

Macrophages are highly versatile immune cells that play pivotal roles in controlling the inflammatory damage that underlies many medical conditions, including auto-immune disorders such as rheumatoid arthritis, cardiovascular diseases, neurodegenerative conditions (such as Alzheimer's or Parkinson's disease), diabetes, and some cancers, to name a few. Macrophages' roles are numerous, and depend strongly upon their 'activation state' or 'phenotype', which can change dynamically in a manner that is dependent upon the inflammatory environment in which they reside (among many other factors) [1,2]. One of the principal roles of macrophages (in their role as the immune system's 'big eaters') is to remove unwanted harmful material (including apoptotic cells) via phagocytosis, in order to minimise the potential for further tissue damage [3]. Alongside this, and depending on their phenotype, macrophages can release either pro- or anti-inflammatory cytokines, with the potential to either worsen or repair inflammatory damage [1,4]. Given that macrophages play such a substantial role in determining the switch between healthy and chronic outcomes for patients, and given that macrophage roles are so strongly linked to the inflammatory environment, understanding the connections between macrophage phenotype switching and resulting inflammatory dynamics is an important goal, especially in the ongoing search for novel therapeutic interventions.

Unambiguously categorising distinct macrophage phenotypes (or polarisation/activation states) is a difficult task, as there is no unique way to quantify a macrophage's polarisation. Instead, macrophage polarisation states are associated with broad categorisations that are implicated based on levels of expression of certain markers, production of certain cytokines, or measures of other cellular functions and properties [5]. Historically, the most common nomenclature has been to divide macrophages into two distinct classes labelled "M1" and "M2"

* Corresponding author.
E-mail address: Martin.Nelson@ntu.ac.uk (M.R. Nelson).

https://doi.org/10.1016/j.mbs.2024.109289

Available online 5 September 2024

(or similarly "classically activated" and "alternatively activated"), with M1 macrophages being linked to pro-inflammatory responses and M2 macrophages being associated with restorative activity [6–9]. However, such categorisations are generally contentious and considered to be overly simplistic descriptions of a much more complex landscape of potential polarisation states. For example, in the context of rheumatoid arthritis, five relevant macrophage subtypes have been identified in *in vitro* assays that consider morphological characteristics, gene expression data related to phenotype markers, and functional aspects including production of Reactive Oxygen Species (ROS) [10]. Increasingly, studies point to the existence of various intermediate or "mixed" macrophage phenotypes that exhibit, for example, some features akin to M1 and some features akin to M2; see, *e.g.* [11–14]. In this sense, we could regard macrophage phenotype as a continuous variable, parameterising a spectrum of states that lie between the M1 and M2 extremes.

Given the complexity of the macrophage phenotype landscape, many previous mathematical models that have sought to understand the dynamics associated with inflammatory conditions have typically incorporated a small, finite number of macrophage phenotypes. In some cases, all macrophages are lumped together as a single 'homogenised' population, which commonly interacts with other cell populations and/or various pro- or anti-inflammatory mediators to determine the resulting inflammatory outcome. Previous works that have taken a homogenisation approach include models of cancers [15,16], stroke [17] and atherosclerosis [18], as well as models that focus upon aspects of the inflammatory response that transfer readily between numerous inflammatory conditions [19–21]. We note, in particular, the work of [22], which used a dynamical systems analysis to study a series of models of inflammation in a generic context, in order to understand which interactions are key in providing bifurcations that underpin switching between resolving and chronic outcomes. Amongst the authors' conclusions was the fact that the rate at which macrophages remove harmful apoptotic cells is a key parameter that drives this switching of outcomes, and is a target for therapeutic manipulation. While the models of [22] used a homogenised approach, with all macrophages assumed restorative, we note that phagocytosis of apoptotic cells is actually primarily attributed to the M2 phenotype, with the M1 phenotype largely being regarded as more deleterious. The models of [22] were later extended to a spatial setting, via partial-differential-equation (PDE) and agent-based approaches, to elucidate the influence of immune cell and mediator motility upon inflammatory dynamics and outcomes [23,24]. Throughout all of these models, macrophage phenotypes do not feature explicitly, and there is hence a risk that the models may over-simplify some key phenotype-specific feedbacks (as described above).

As our understanding of disparate macrophage phenotypes has continued to advance over recent years, increasingly mathematical models have gone beyond the homogenisation approach to include two or more distinct phenotypes. Examples of such models can be found in contexts including inflammatory bowel disease [25], hepatitis [26,27], asthma [28], and cancer [29–31], to list just a few. More recently, in [32], we presented extensions of the models of [22] to include two populations of macrophages of opposing phenotypes (referred to as pro- and anti-inflammatory macrophages, but loosely representative of the M1/M2 categorisation). Taking a systematic approach, we presented a series of models of increasing complexity, starting with a model of a homogenised macrophage population, before building to a two-macrophage-phenotype model, and finally supplementing this with additional feedbacks from a coexistent population of neutrophils. Moving from each model to the next, we examined changes in the bifurcation structures of the models as new feedbacks were added, in order to understand the role each model interaction has in determining the resulting dynamics and the switch between chronic and healthy outcomes. Our analysis revealed that incorporating two distinct macrophage phenotypes resulted in additional oscillatory solutions (reminiscent of inflammatory conditions that exhibit relapsing–remitting characteristics) not observed in the previous models of [22]. These oscillatory solutions were most evident for large macrophage populations, for which there is scope for larger disparity between the numbers of macrophages of each phenotype. Furthermore, rates of macrophage phenotype switching were shown to impact resulting outcomes in a largely intuitive manner; high rates of switching toward the restorative phenotype can eliminate chronic outcomes entirely, and high rates of switching toward the pro-inflammatory phenotype can both worsen chronic outcomes and promote further chronic configurations through increased multistability. We note that these findings are consistent with the fact that active manipulation of macrophage phenotype is one area of focus in treatment of various inflammatory conditions [33,34].

While the two-phenotype models of [32] do make progress toward a better understanding of the dynamics underlying inflammatory conditions, we note that this perspective still represents a degree of over-simplicity that omits the influence of 'intermediate' phenotypes. We seek to address this here. While some previous models have explicitly included discrete intermediate or mixed phenotypes (e.g. [29,30]), models that incorporate a continuum description of macrophage phenotypes are comparatively sparse. In [35], in order to understand the roles of heterogeneous macrophage populations upon solid tumour aggregation, two models are presented and compared: one which takes a two-phenotype (pro-tumour and anti-tumour) approach, and one which considers a macrophage population that is structured according to a continuous phenotype variable. These models were compared via steady state analysis and numerical simulation; while numerical simulations were similar between these approaches, the two-phenotype model was shown to exhibit greater multistability. The interactions of heterogeneous macrophage populations with tumours have also been modelled via agent-based approaches, which can include continuous descriptions of polarisation states [36,37]. We note that, to our knowledge, no authors have to date interrogated a continuum-based description of macrophage polarisation states via an approach of formal bifurcation analysis; this approach forms the focus of our work here.

In this article, we develop a new PDE-based extension of the two-phenotype models of [32] that utilises a continuous description of macrophage polarisation states that accounts for intermediate phenotypes. For simplicity, we restrict attention to the interactions of macrophages with background inflammatory mediators, and neglect the roles of other immune cells here. Our model incorporates a spectrum of phenotype configurations that ranges between extreme configurations representing fully pro-inflammatory (M1) and fully anti-inflammatory (M2) phenotypes, and model phenotype switching via convective flux terms whose magnitudes scale under the influence of generic populations of pro- and anti-inflammatory mediators, which together provide a description of the inflammatory environment in which our macrophage population resides. We analyse our model through numerical simulation (conducted in Matlab) and dynamical systems analysis (including via the numerical continuation package XPPAUT, as described in [38,39]). Supporting Matlab and XPPAUT codes are provided online[1] in order to facilitate re-use of this model in future inflammation studies that may, for example, include more detailed descriptions of inflammatory mediators or incorporate other immune cells. Throughout our analysis, we are interested in the extent to which key cellular and mediator interactions provide switches between resolving and chronic outcomes via corresponding bifurcations, and the extent to which this switching of outcomes is influenced by shifts in macrophage phenotype. Throughout, we pay close attention to the extent to which our macrophage population is polarised toward pro- or

[1] See github.com/martinrnelson/MacrophageContinuum.

Table 1
Summary of the dependent variables appearing in our model, with corresponding units.

Variable	Meaning	Units
m^*	Macrophage density (per tissue volume)	cells mm^{-3}
g^*	Anti-inflammatory mediator concentration	pg mm^{-3}
c^*	Pro-inflammatory mediator concentration	pg mm^{-3}

anti-inflammatory phenotypes, and the corresponding role of intermediate phenotypes that do not feature in the previous models of [32]. To conclude, we reflect on our dynamical systems observations in the context of the ongoing search for therapeutic interventions in a range of inflammatory conditions.

2. Model

We model macrophages on a continuous spectrum of phenotypes, classified according to their levels of pro/anti-inflammatory activity. We denote the number of macrophages by $m^*(t^*, p)$, where t^* represents time and stars are used to distinguish dimensional variables from their dimensionless counterparts below. The independent variable $p \in [-1, 1]$ here parameterises macrophage phenotypes, with $p = 1$ corresponding to a fully pro-inflammatory phenotype and $p = -1$ corresponding to a fully anti-inflammatory phenotype. Additionally, we introduce variables $c^*(t^*)$ and $g^*(t^*)$ to represent concentrations of generic pro- and anti-inflammatory mediators present in the tissue of interest; thus, c^* and g^* together describe the inflammatory landscape in which macrophages reside. (The dependent variables appearing in our model are also summarised in Table 1.) We expect macrophages to switch phenotype dynamically in response to changes in the inflammatory context, with high levels of inflammation (c^* high, g^* low) driving a shift toward pro-inflammatory macrophage phenotypes, and low levels of inflammation promoting a shift to the anti-inflammatory phenotypes typically found in resident macrophage populations in healthy tissues [40]. A schematic illustration of the interactions included in our model is shown in Fig. 1.

We model phenotype switching via two convective fluxes, $\mathbf{q}^{+*}$ and $\mathbf{q}^{-*}$, which shift macrophages toward pro-inflammatory and anti-inflammatory phenotypes respectively. We expect pro-inflammatory mediators, c^*, to drive macrophages to become more pro-inflammatory, and expect the strength of the corresponding flux to be largest for fully anti-inflammatory macrophages (with $p = -1$), with macrophages at the fully pro-inflammatory end of the phenotype spectrum ($p = 1$) not being affected at all. Thus, we write

$$\mathbf{q}^{+*} = \alpha_1^* c^* (1 - p)\, m^*. \tag{1}$$

Similarly, anti-inflammatory mediators, g^*, drive phenotypic switching in the opposing direction, with the greatest effect on macrophages with $p = 1$. We write

$$\mathbf{q}^{-*} = -\alpha_2^* g^* (1 + p)\, m^*. \tag{2}$$

Here, the parameters α_1^* and α_2^* describe the rates of phenotypic switching in response to environmental cues from mediators. We also note that these choices of flux terms constrain macrophages to the domain $p \in [-1, 1]$, since $\mathbf{q}^{+*}$ is zero when $p = 1$ and $\mathbf{q}^{-*}$ is zero when $p = -1$.

Following [32], we assume that macrophages proliferate logistically up to some maximum population size m^*_{max} (which we expect to vary between tissues), and that the rate of proliferation is enhanced in the presence of pro-inflammatory mediators (c^*). Additionally, we incorporate macrophage loss (due to either cell death or migration away from the tissue of interest) at a constant rate γ_m^*. Thus, we have the following partial differential equation that governs the macrophage population:

$$\frac{\partial m^*}{\partial t^*} + \frac{\partial}{\partial p}\left(\alpha_1^* c^* (1 - p)\, m^* - \alpha_2^* g^* (1 + p)\, m^*\right)$$
$$= k^* \left(c^* + c_T^*\right) R(p) m_T^* \left(1 - \frac{m_T^*}{m_{max}^*}\right) - \gamma_m^* m^*, \tag{3}$$

in which $k^* c_T^*$ is the baseline rate of macrophage proliferation in the absence of pro-inflammatory mediators, $R(p)$ is a function specifying which phenotypic configuration newly acquired macrophages reside in (specified in Section 3 below), and $m_T^*(t^*)$ is the total number of macrophages present in the system at a given time, given by:

$$m_T^*\left(t^*\right) = \int_{-1}^{1} m^*\left(t^*, p\right) \mathrm{d}p. \tag{4}$$

To prescribe mediator dynamics, we take the interactions given in the models of [32] as a guide, noting that macrophages can produce both pro- and anti-inflammatory mediators (in a manner that depends on their phenotype). Our mediator dynamics are governed by the following ordinary differential equations:

$$\frac{\mathrm{d}g^*}{\mathrm{d}t^*} = \kappa_g^* \int_{-1}^{1} f_1(p) m^* \mathrm{d}p - \gamma_g^* g^*, \tag{5}$$

$$\frac{\mathrm{d}c^*}{\mathrm{d}t^*} = \kappa_c^* \int_{-1}^{1} f_2(p) m^* \mathrm{d}p - \delta^* c^* g^* - \gamma_c^* c^*, \tag{6}$$

in which κ_g^* and κ_c^* parameterise rates of mediator production, γ_g^* and γ_c^* parameterise rates of mediator decay, δ^* represents a mitigating effect of anti-inflammatory mediators against pro-inflammatory mediators, and the functions $f_1(p)$ and $f_2(p)$ describe how the rates of production of each group of mediators varies as a function of macrophage phenotype. For simplicity, we assume linear dependences for the latter, *i.e.*

$$f_1(p) = \frac{1 - p}{2}, \qquad f_2(p) = \frac{1 + p}{2}; \tag{7}$$

that is, macrophages that are in a fully pro-inflammatory configuration ($p = 1$) produce no anti-inflammatory mediators at all and, likewise, macrophages that are fully anti-inflammatory ($p = -1$) produce no pro-inflammatory mediators.

We solve the system (3)–(7) subject to initial conditions representing an initially positive population of macrophages and some appropriate mediator concentrations. We therefore prescribe

$$m = m_0^*(p), \qquad c^* = c_0^*, \qquad g^* = g_0^* \qquad \text{at } t^* = 0. \tag{8}$$

2.1. Nondimensionalisation

To simplify our analysis below, we nondimensionalise (3)–(8) by introducing the following scalings:

$$t^* = \frac{1}{\gamma_c^*} t, \qquad g^* = \frac{\gamma_c^*}{\delta^*} g, \qquad c^* = \frac{\gamma_c^*}{k^*} c, \qquad m^* = \frac{\gamma_c^{*2}}{\delta^* \kappa_g^*} m, \tag{9}$$

which yields the following system of dimensionless equations:

$$\frac{\partial m}{\partial t} + \frac{\partial}{\partial p}\left(\alpha_1 c\,(1 - p)\, m - \alpha_2 g\,(1 + p)\, m\right)$$
$$= \left(c + c_T\right) R(p) m_T \left(1 - \frac{m_T}{m_{max}}\right) - \gamma_m m, \tag{10}$$

$$\frac{\mathrm{d}g}{\mathrm{d}t} = \int_{-1}^{1} f_1(p) m\, \mathrm{d}p - \gamma_g g, \tag{11}$$

$$\frac{\mathrm{d}c}{\mathrm{d}t} = \kappa_c \int_{-1}^{1} f_2(p) m\, \mathrm{d}p - c g - c, \tag{12}$$

with

$$m_T(t) = \int_{-1}^{1} m(t, p) \mathrm{d}p. \tag{13}$$

In (10)–(12) above, we have introduced the following dimensionless parameter groupings:

$$\gamma_g = \frac{\gamma_g^*}{\gamma_c^*}, \qquad \gamma_m = \frac{\gamma_m^*}{\gamma_c^*}, \qquad \kappa_c = \frac{\kappa_c^* k^*}{\kappa_g^* \delta^*}, \qquad c_T = \frac{k^* c_T^*}{\gamma_c^*} \tag{14}$$

$$\alpha_1 = \frac{\alpha_1^*}{k^*}, \qquad \alpha_2 = \frac{\alpha_2^*}{\delta^*}, \qquad m_{max} = \frac{\delta^* \kappa_g^* m_{max}^*}{\gamma_c^{*2}}. \tag{15}$$

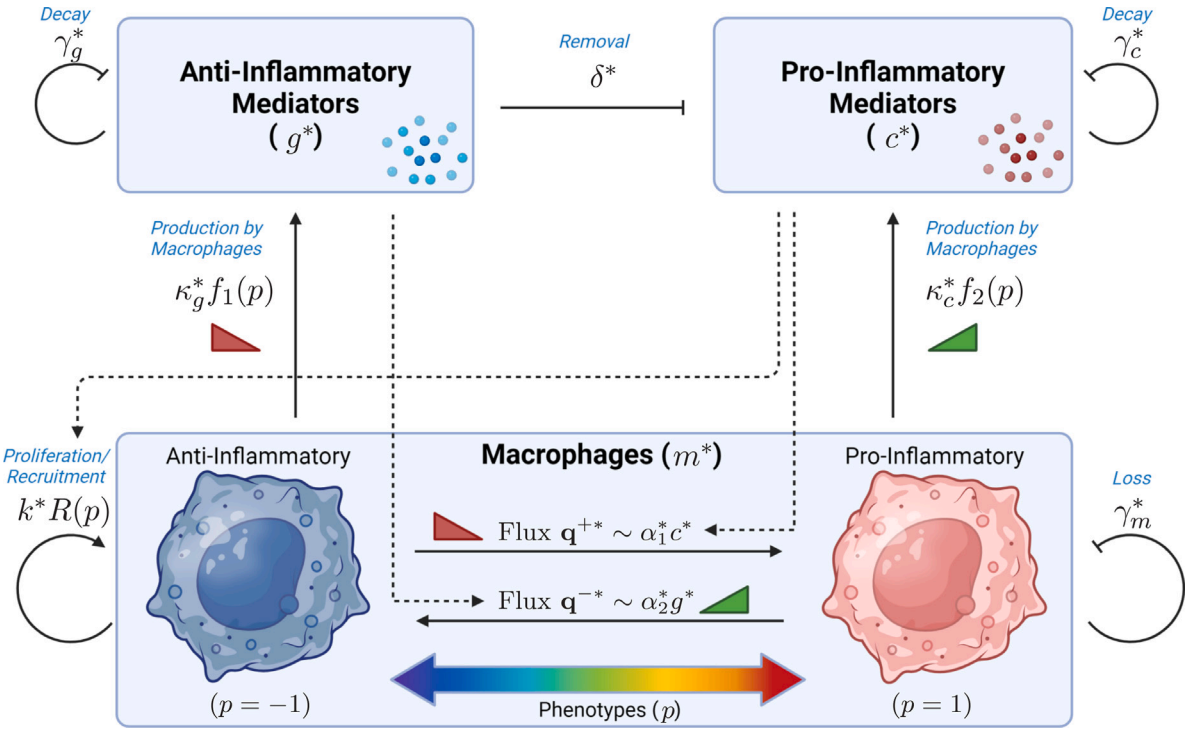

Fig. 1. Schematic illustration of the interactions included in our model. Arrows indicate production terms or positive fluxes, lines terminated with bars represent loss terms, and dashed arrows indicate that corresponding macrophage behaviours scale with environmental cues represented by relevant mediator concentrations. Green/red triangles respectively indicate feedbacks whose strength increases/decreases with the phenotype variable p.

We solve (10)–(13) subject to the initial conditions:

$$m = m_0(p), \qquad c = c_0, \qquad g = g_0 \qquad \text{at } t = 0. \tag{16}$$

2.2. Parameters

A summary of the dimensional parameters appearing in our model is provided in Table 2. We note that theoretical studies of inflammation, in general, suffer from difficulties in accurately inferring corresponding model parameters due to limitations in available experimental data. This is due to a variety of factors, including a lack of suitable non-invasive experimental protocols, the fact that parameter values would be likely to have significant variability between differing inflammatory conditions and affected tissues, and due to patients with inflammatory conditions commonly reporting late to medical professionals, limiting the extent to which the onset of the acute inflammatory phase can be interrogated. Furthermore, we note that inferring rate parameters, in particular, would require temporal data that is difficult to obtain *in vivo*. In light of these limitations, it is more practical to estimate the orders of magnitude of corresponding dimensionless parameter groupings based on our knowledge of which mechanisms dominate. Our approach is to construct a baseline set of dimensionless parameter values (given in Table 3) which reflects available knowledge around dominant mechanisms, and to then analyse the impact of variations in these parameters via numerical simulation and bifurcation analysis. Where possible, we configure our baseline parameter choices to be consistent with those of [32], in order to facilitate comparison of the PDE model discussed here with related ODE models discussed in [32].

The decay rates of individual mediators are reasonably well documented, but can vary according to the medical context in question. For example, the half-lives of the pro-inflammatory cytokines IL–1β, IL–8 and TNFα have been indicated to lie in the range 18.2–24 min, while the anti-inflammatory cytokine IL–1RA decays more slowly with a half-life in the range 4–6 h [41]. In our model, this could suggest that $\gamma_g = \gamma_g^*/\gamma_c^* \ll 1$. However, some cytokines (*e.g.* IL–6) can have both pro- and anti-inflammatory effects [41], suggesting that $\gamma_g \sim 1$ in some contexts. Here, following [32], we take $\gamma_g = 0.2$ as our default value in Table 3.

Identifying accurate values for the parameters that govern macrophage population dynamics is difficult in general, since these depend upon the scale of the affected tissue. However, the rate of macrophage loss (γ_m^*) has been documented (in the context of wound healing) to lie in the range 0.2–1.41 per day [42,43], indicating that macrophage loss occurs at a slower rate than decay of pro-inflammatory mediators; we hence set $\gamma_m = \gamma_m^*/\gamma_c^* < 1$ in Table 3. Accurately prescribing the rate of proliferation/recruitment of the macrophage populations in isolation is hindered by the fact that macrophage proliferation rates are known to depend on background levels of inflammatory mediators [44]. In (10), we assume that macrophage proliferation rates take a linear dependence upon pro-inflammatory mediator concentrations (*i.e.* of the form $c + c_T$) and, under the expectation that proliferation rates should appreciably increase in the presence of pro-inflammatory mediators, we expect c_T to be small in comparison to the scale over which c varies. We therefore set $c_T = 0.01$ in Table 3. Likewise, since the maximal macrophage population size will depend heavily on the size of the tissue of interest, we follow [32] in choosing $m_{max} = 25$ as a baseline value in Table 3.

We expect macrophage phenotype switching toward the pro-inflammatory end of the spectrum (α_1) to dominate the converse direction (α_2) as many inflammatory conditions are associated with increased ratios of pro-inflammatory macrophages [45,46]; thus we expect $\alpha_1 \gg \alpha_2$ in general.

The remaining mediator production rate parameter, κ_c, is not readily available from existing literature. Following [32], we choose $\kappa_c = 0.35$ as our baseline value; however, we note that our definition of κ_c here varies slightly from that of [32], since its interpretation here is inherently linked to the manner in which the mediator production functions $f_2(p)$ and, indirectly, $f_1(p)$ are prescribed. Here, we choose $f_1(p)$ and $f_2(p)$ to be $\mathcal{O}(1)$ functions, and vary the strength of the production of mediators via κ_c. Variations of all parameter values around these baseline values are examined throughout our analyses below.

Table 2
Summary of the dimensional parameters appearing in the model, with corresponding units.

Parameter	Meaning	Units
Macrophage parameters		
k^*	Rate of (logistic) growth of macrophage population	$\mathrm{mm^3\,pg^{-1}\,day^{-1}}$
c_T^*	Pro-inflammatory mediator concentration at which macrophage proliferation is at its minimal rate	$\mathrm{pg\,mm^{-3}}$
m_{max}^*	Maximum size of macrophage population	$\mathrm{cells\,mm^{-3}}$
α_1^*	Rate of macrophage phenotype switching toward pro-inflammatory phenotypes	$\mathrm{mm^3\,pg^{-1}\,day^{-1}}$
α_2^*	Rate of macrophage phenotype switching toward anti-inflammatory phenotypes	$\mathrm{mm^3\,pg^{-1}\,day^{-1}}$
γ_m^*	Rate of loss of macrophages (all phenotypes)	$\mathrm{day^{-1}}$
Anti-inflammatory mediator parameters		
κ_g^*	Rate of production by macrophages	$\mathrm{pg\,cell^{-1}\,day^{-1}}$
γ_g^*	Decay rate	$\mathrm{day^{-1}}$
Pro-inflammatory mediator parameters		
κ_c^*	Rate of production by macrophages	$\mathrm{pg\,cell^{-1}\,day^{-1}}$
γ_c^*	Decay rate	$\mathrm{day^{-1}}$
δ^*	Rate of loss due to mitigating effect of anti-inflammatory mediators	$\mathrm{mm^3\,pg^{-1}\,day^{-1}}$

Table 3
Summary of the dimensionless parameters appearing in the model. Parameter values are estimated as described in Section 2.2.

Parameter	Expression	Meaning	Baseline value
κ_c	$k^*\kappa_c^*/\delta^*\kappa_g^*$	Rate of production of pro-inflammatory mediators	0.35
γ_m	γ_m^*/γ_c^*	Decay of macrophages	0.05
γ_g	γ_g^*/γ_c^*	Decay of anti-inflammatory mediators	0.2
c_T	$k^*c_T^*/\gamma_c^*$	Rate of macrophage proliferation in the absence of c	0.01
m_{max}	$\delta^*\kappa_g^*m_{max}^*/\gamma_c^{*2}$	Maximum macrophage population size	25
α_1	α_1^*/k^*	Macrophage phenotype switching (anti to pro)	1
α_2	α_2^*/δ^*	Macrophage phenotype switching (pro to anti)	0.01

3. Results

In the following sections, we use a combination of numerical simulations conducted in Matlab and bifurcation analyses conducted in XPPAUT to analyse the system (10)–(13). In both cases, the corresponding codes involve a finite difference discretisation in the phenotype variable p, which converts our PDE system into a system of ODEs that can be simulated using standard in-built solvers. More details of the numerical scheme are given in Appendix. Throughout, we are interested in whether (for a given set of parameter values) the system admits a positive steady state that represents chronic inflammation, returns to a 'healthy' steady state in which pro-inflammatory components are zero, or provides more complex dynamics such as oscillatory solutions (which could be likened to inflammatory conditions that exhibit relapsing–remitting characteristics). We will observe that, often, the system may exhibit multiple of these potential solutions for a fixed parameter set, with the switch between outcomes being governed by initial conditions. We will also draw comparisons of the results of this PDE model against earlier models that have less detailed descriptions of macrophage phenotypes to elucidate the extent to which our conclusions may be sensitive to the modelling approach.

3.1. Stability of the zero state

It is trivial to see that the system (10)–(13) has a steady state at $m = g = c = 0$. Since this steady state contains no pro-inflammatory components, we regard this configuration as one type of resolved outcome. In order to determine the stability of this steady state, we linearise (10)–(13) by introducing the following scalings:

$$m(t,p) = \varepsilon\hat{m}(t,p), \qquad g(t) = \varepsilon\hat{g}(t), \qquad c(t) = \varepsilon\hat{c}(t), \tag{17}$$

and write

$$m_T = \varepsilon\int_{-1}^{1}\hat{m}(t,p)\,\mathrm{d}p = \varepsilon\hat{m}_T. \tag{18}$$

At $\mathcal{O}(\varepsilon)$, (10)–(12) reduce to

$$\frac{\partial\hat{m}}{\partial t} = c_T R(p)\hat{m}_T - \gamma_m\hat{m}, \tag{19}$$

$$\frac{\mathrm{d}\hat{g}}{\mathrm{d}t} = \int_{-1}^{1} f_1(p)\hat{m}\,\mathrm{d}p - \gamma_g\hat{g}, \tag{20}$$

$$\frac{\mathrm{d}\hat{c}}{\mathrm{d}t} = \kappa_c\int_{-1}^{1} f_2(p)\hat{m}\,\mathrm{d}p - \hat{c}. \tag{21}$$

For the linear choices of $f_1(p)$ and $f_2(p)$ given in (7), we can simplify the integrals in (20) and (21) by noting the following (in which we write $f(p)$ in place of $f_1(p)$ or $f_2(p)$ for compactness):

$$\begin{aligned}\int_{-1}^{1} f(p)\hat{m}\,\mathrm{d}p &= \frac{1}{2}\int_{-1}^{1}(1\pm p)\,\hat{m}\,\mathrm{d}p\\ &= \frac{1}{2}\int_{-1}^{1}\hat{m}\,\mathrm{d}p \pm \frac{1}{2}\int_{-1}^{1}p\hat{m}\,\mathrm{d}p\\ &= \frac{1}{2}\hat{m}_T \pm \frac{1}{2}\left(p\hat{m}_T\Big|_{-1}^{1} - \int_{-1}^{1}\hat{m}_T\,\mathrm{d}p\right).\end{aligned} \tag{22}$$

Noting that $\hat{m}_T$ is independent of p, the bracketed terms in (22) cancel and we have

$$\int_{-1}^{1} f(p)\hat{m}\,\mathrm{d}p = \frac{1}{2}\hat{m}_T. \tag{23}$$

Since (23) reveals that (20) and (21) depend only upon $\hat{m}_T$, rather than $\hat{m}$ itself, it is helpful to reformulate (19) in terms of $\hat{m}_T$ and eliminate $\hat{m}$ entirely. We note that

$$\begin{aligned}\frac{\mathrm{d}\hat{m}_T}{\mathrm{d}t} &= \frac{\mathrm{d}}{\mathrm{d}t}\int_{-1}^{1}\hat{m}\,\mathrm{d}p\\ &= \int_{-1}^{1}\frac{\partial\hat{m}}{\partial t}\,\mathrm{d}p\\ &= \int_{-1}^{1} c_T R(p)\hat{m}_T - \gamma_m\hat{m}\,\mathrm{d}p,\end{aligned} \tag{24}$$

in which the final equality comes from (19). Restricting attention to the case $R(p) = 1$ for ease, (24) then provides

$$\frac{\mathrm{d}\hat{m}_T}{\mathrm{d}t} = c_T\int_{-1}^{1}\hat{m}_T\,\mathrm{d}p - \gamma_m\int_{-1}^{1}\hat{m}\,\mathrm{d}p = \left(2c_T - \gamma_m\right)\hat{m}_T, \tag{25}$$

in which we have again noted that $\hat{m}_T$ is independent of p.

With (25) replacing (19), and with (20) and (21) rewritten according to (23), (19)–(21) can be expressed as the following linear system:

$$\frac{\mathrm{d}}{\mathrm{d}t}\begin{pmatrix}\hat{m}_T\\ \hat{g}\\ \hat{c}\end{pmatrix}=\underbrace{\begin{pmatrix}2c_T-\gamma_m & 0 & 0\\ \frac{1}{2} & -\gamma_g & 0\\ \frac{\kappa_c}{2} & 0 & -1\end{pmatrix}}_{\mathbf{J}}\begin{pmatrix}\hat{m}_T\\ \hat{g}\\ \hat{c}\end{pmatrix}. \tag{26}$$

Since the Jacobian matrix **J** is triangular, its eigenvalues are given by its diagonal entries. For the zero state to be stable, we require all the eigenvalues of **J** have negative real part. Thus, the zero state is stable provided that

$$c_T < \frac{\gamma_m}{2}. \tag{27}$$

The stability of the zero state is therefore determined by the underlying growth/decay dynamics of the macrophage population in the absence of inflammatory stimuli, with c_T representing the rate of growth of the macrophage population in the absence of pro-inflammatory mediators, and γ_m being the rate of loss of macrophages as they vacate the tissue or die.

3.2. Solutions for $R(p) = 1$

For simplicity, we begin our numerical analysis with consideration of the case $R(p) = 1$, for which all macrophage phenotypes are recruited uniformly. While this is not necessarily a biologically realistic assumption, it provides a useful starting point for our mathematical analysis; we examine the impact of non-uniform choices of $R(p)$ in Section 3.3 below.

Fig. 2 illustrates some typical solutions to (10)–(13). Here, we hold all parameters fixed at the values of Table 3 but vary γ_g to illustrate the range of permissible solutions. For $\gamma_g = 1$ (Fig. 2(a)), the system attains a steady state configuration in which pro-inflammatory mediator concentrations are high, anti-inflammatory mediator concentrations are low, and macrophages are polarised entirely toward pro-inflammatory phenotypes. This configuration represents a chronic inflammatory outcome. Reducing γ_g to its default value of 0.2 (Fig. 2(b)), results in higher levels of anti-inflammatory mediators, which stimulates macrophage phenotype switching toward anti-inflammatory phenotypes (via the flux term arising from (2)). Here, the system attains a stable oscillatory configuration (periodic orbit) with macrophages mostly polarised toward anti-inflammatory activity but also with periodic surges of more pro-inflammatory phenotypes that prevent the inflammation being mitigated against entirely. Levels of pro-inflammatory mediators are lower than in Fig. 2(a) due to the upscaled role of the anti-inflammatory mediators and macrophages, but the solution is nonetheless chronic. In Fig. 2(c), we set $\gamma_g = 0.01$ and observe that, while pro-inflammatory mediator concentrations are initially sufficiently high to drive macrophages toward pro-inflammatory phenotypes, rapid accumulation of anti-inflammatory mediators then reverses the direction of phenotypic switching, moving macrophages toward anti-inflammatory configurations. Here, pro-inflammatory mediator concentrations eventually reach zero and the macrophage population ultimately leaves the tissue entirely as the macrophage decay term via γ_m outweighs the growth term (c_T) in (10); the system reaches the zero state, which is stable for these parameter choices according to (27). We regard this configuration as a healthy outcome in which inflammation is resolved entirely.

We note that, in Fig. 2, we have illustrated typical outcomes by varying one of our model parameters (γ_g in this case). Equally, for some parameters, we could illustrate similar results by holding parameters fixed and varying our initial conditions, since the model is bistable for many parameter choices. In order to elucidate how our model's solutions depend on each of our parameters more fully, we perform bifurcation analyses in XPPAUT to track the coordinates of steady states and oscillatory solutions as a function of each parameter. (See Appendix for further details of the numerical scheme used; the corresponding XPPAUT code is also available online.) Fig. 3 illustrates bifurcation diagrams for each of our seven model parameters, holding all unspecified parameters at the values given in Table 3. The vertical axes in the figures show the pro-inflammatory mediator concentration, c, which is a proxy for the severity of chronically inflamed states. The inset figures in the top-right of each panel provide an indication of the corresponding macrophage phenotypes for each branch; colouring represents the 'median' macrophage phenotype, calculated according to

$$p_{median} = \min \hat{p} \in [-1, 1] : \int_{-1}^{\hat{p}} m \, \mathrm{d}p \geq \frac{m_T}{2}, \tag{28}$$

with configurations for which $m_T = 0$ coloured black. Dark blue or dark red colourings indicate that the distribution of macrophage phenotypes is mostly anti-inflammatory or mostly pro-inflammatory, respectively. In the case of periodic solutions, we colour branches by evaluating (28) at the points of the orbit at which the pro-inflammatory mediator concentrations are highest and lowest; the difference in colour between the upper and lower branches indicates the extent to which the 'median phenotype' shifts during each oscillatory cycle.

Table 4
Abbreviations used in annotations of Figs. 3 and 4.

Abbreviation	Description
(Res)	Resolution: the only stable solution is the steady state at zero
(Chr)	Chronic: the only stable solution is a single chronic steady state
(B)	The model is bistable with both resolving and chronic steady states permissible
(Multi)	The model permits more than two stable steady states, one of which is the zero state
(Res/Osc)	The model converges to either the zero state or an oscillatory solution
(B/Osc)	The model converges to either the zero state, a unique chronic state or an oscillatory solution
(Chr:2)	The model has two stable chronic steady states; the zero state is unstable

For the parameter values of Table 3, the model permits resolution via convergence to the zero state (as per (27), labelled "Res" in Fig. 3), or chronic oscillatory outcomes as shown in Fig. 2(b) (labelled "Osc" in Fig. 3). In general, we observe that changes in parameter values that stimulate macrophage numbers, either directly (γ_m smaller, or c_T larger) or indirectly via pro-inflammatory mediators (κ_c larger), can act to overwhelm oscillations, eliminating them via a Hopf bifurcation and often giving rise to a chronic steady state. Furthermore, increasing c_T and/or reducing γ_m can destabilise the zero state via a transcritical bifurcation corresponding to (27), resulting in a configuration of the model in which a chronic steady state outcome is guaranteed (demarked by "Chr" in Fig. 3). Conversely, increasing γ_m or decreasing c_T (both of which reduce the size of the macrophage population) results in a growth of the amplitude of oscillatory solutions, until the periodic orbit ultimately collides with a neighbouring saddle (with $c \simeq 0$) and is hence eliminated via a homoclinic bifurcation. For sufficiently large choices of γ_m, in particular, the only permissible solution is one of resolution, the zero state being the only stable solution here. Intuitively, we may make converse conclusions regarding stimulation or repression of anti-inflammatory mediators, in comparison to those of pro-inflammatory mediators: for γ_g small, we have large numbers of anti-inflammatory mediators and chronic outcomes are eliminated; oscillations exist for values of γ_g lying between a Hopf bifurcation and a homoclinic bifurcation; and moderate to large choices of γ_g (for which anti-inflammatory mediator contributions are lesser) reveal regions of bistability or multistability (labelled "B" and "Multi" in Fig. 3) in which there are two or more stable steady states and the system may attain either resolved or chronic steady-state outcomes.

The existence of oscillatory solutions requires a reasonably large macrophage population, oscillations being eliminated entirely for m_{max}

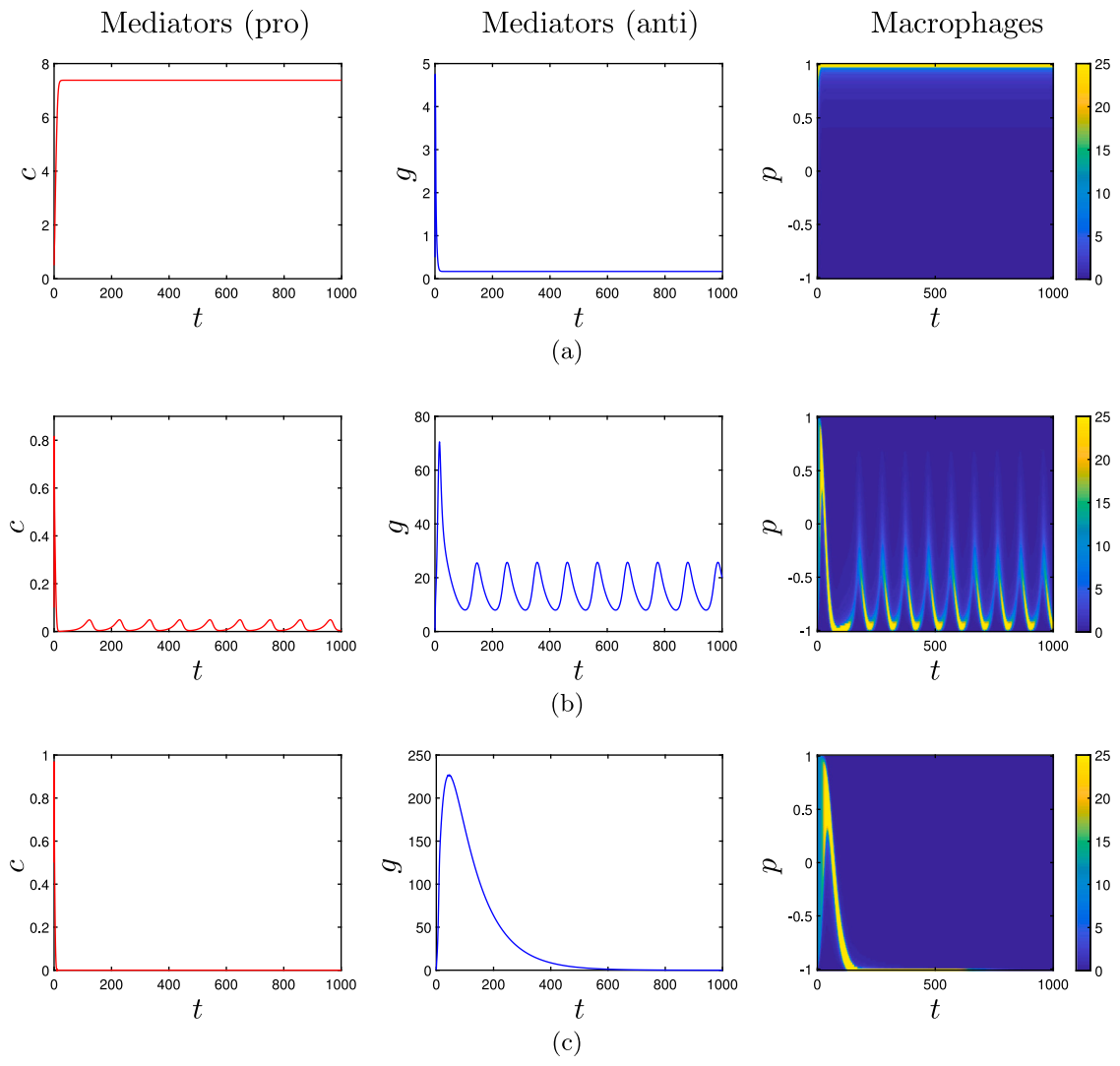

Fig. 2. Numerical simulations of (10)–(13) subject to initial conditions $c(0) = g(0) = 0.5$ and $m(0, p) = 10$ for (a) $\gamma_g = 1$, (b) $\gamma_g = 0.2$ and (c) $\gamma_g = 0.01$, $R(p) = 1$ and all unspecified parameters as given in Table 3. In each row, we show the pro-inflammatory mediator concentrations ($c(t)$, left), the anti-inflammatory mediator concentrations ($g(t)$, centre) and the distribution of macrophage phenotypes ($m(t, p)$, right). In the right-hand panels, the colour-bar represents the number density of each macrophage phenotype, with anti-inflammatory phenotypes at the base of the figures ($p = -1$) and pro-inflammatory phenotypes at the top of the figures ($p = 1$). In (a) and (c), the model approaches steady states with macrophages polarised toward pro- and anti-inflammatory phenotypes respectively, while in (b) the model attains an oscillatory solution that includes a distribution of intermediate phenotypes but with polarisation biased toward anti-inflammatory activity.

small. This observation is consistent with the findings of corresponding ODE models given by [32]; see *e.g.* Figure 6(b) of [32]. Furthermore, we observe that oscillatory solutions generally correspond to macrophage configurations that comprise primarily anti-inflammatory and intermediate phenotypes; large numbers of strongly pro- inflammatory macrophage phenotypes generally correspond to the existence of stable chronic steady states. In some sense, we may liken our observed oscillatory solutions to conditions with relapsing–remitting characteristics; while a typical periodic orbit includes phases where the macrophage population is almost entirely polarised at or close to the anti-inflammatory end of the spectrum ($p = -1$), inflammatory flare-ups arise concordant with surges in the numbers of intermediate macrophage phenotypes that are more pro-inflammatory in nature (an example of which is shown in Fig. 3(b)).

The phenotype switching parameters, α_1 and α_2, play a joint role in controlling many of the above observations. For α_1 fixed at its default value of Table 3, varying α_2 reveals a window of α_2–values in which oscillations exist, bounded between two Hopf bifurcations. (See Fig. 3(d).) For α_2 fixed at its default value, smaller choices of α_1 result in a bistable configuration in which the model attains either the zero state or a weakly-inflamed chronic state that is mitigated by macrophage polarisation toward anti-inflammatory phenotypes. Meanwhile, larger choice of α_1 can give rise to a new chronic state in which pro-inflammatory mediator concentrations are much higher and macrophages are primarily polarised toward pro-inflammatory phenotypes (as shown in Fig. 3(c)). In order to fully understand the joint effect of these two parameters (and others), it is helpful to track the coordinates of the bifurcations observed above in two-dimensional slices of parameter space, as illustrated in Fig. 4.

Fig. 4 illustrates various two-parameter bifurcation diagrams that reveal a reasonably complex interdependence between our model parameters, illustrating numerous areas of parameter space in which model outcomes are distinct. Here, we place particular focus upon the parameters γ_m (which indirectly controls the size of the macrophage population and influences the scope for resolution via (27)), α_1 and α_2 (which control phenotype switching), and κ_c and γ_g (which together govern the scales of supporting inflammatory mediators). While two-parameter bifurcation diagrams involving other parameter combinations were examined, these are omitted for brevity here since they did not reveal any additional novel dynamics not otherwise captured in

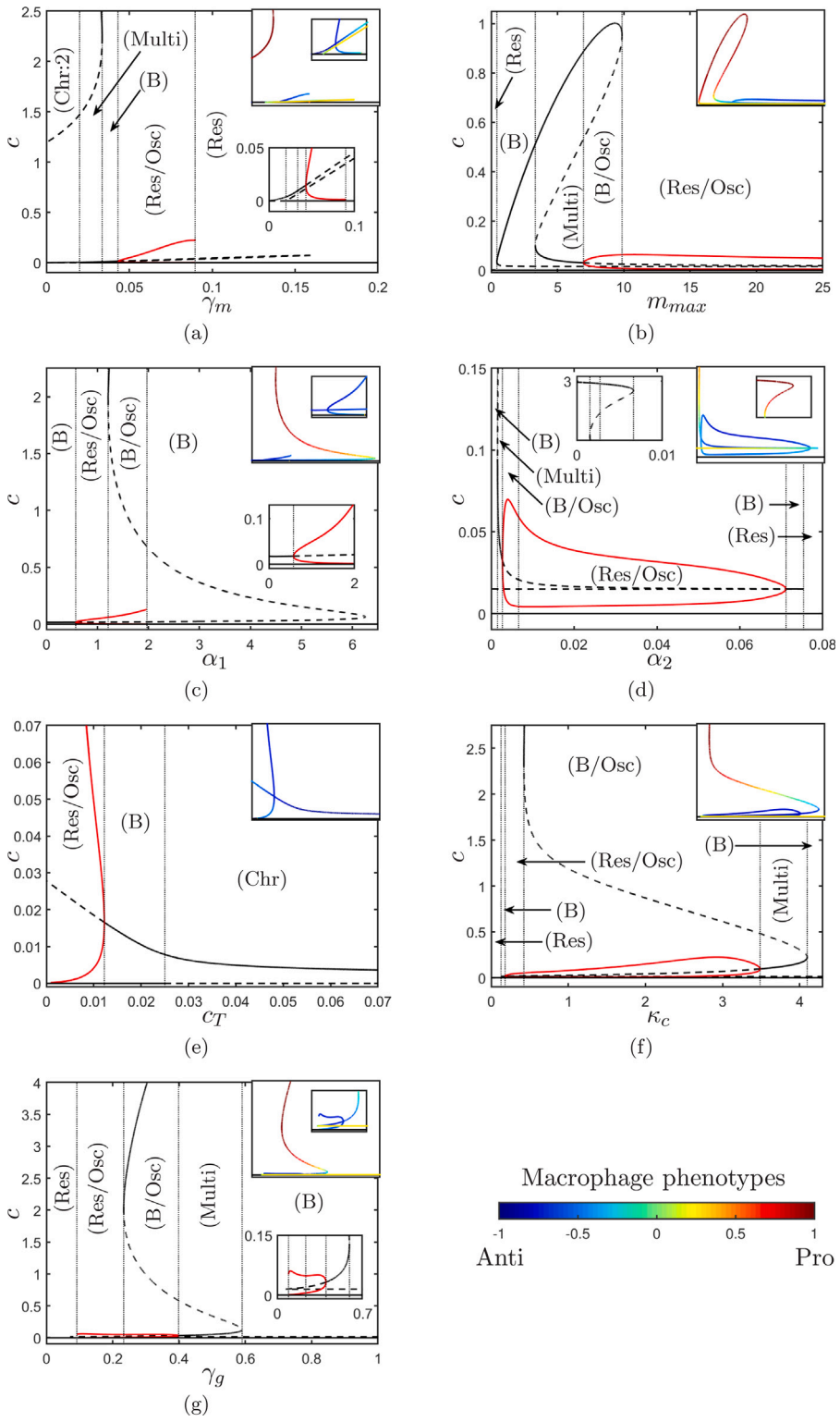

Fig. 3. Bifurcation diagrams illustrating solutions of (10)–(13). All unspecified parameters are as in Table 3. Solid/dashed curves represent stable/unstable solutions; black and red represent steady states and periodic orbits respectively. Inset: the same curves, but instead coloured according to the median macrophage phenotype given by (28). A list of abbreviations is given in Table 4.

Fig. 4. In Fig. 4(a,b), we expose how the macrophage phenotype switching parameters (α_1 and α_2) act in tandem with the rate of macrophage decay (γ_m) to control the location of corresponding bifurcations. From (27), we know that the zero state (which corresponds to resolution of inflammation) is destabilised via a transcritical bifurcation at $\gamma_m = 0.02$ (for the parameter values of Table 3). This transcritical bifurcation is shown as blue curves in Fig. 4(a,b). To the left of these curves, γ_m is relatively small and the macrophage population is relatively large, and the model is relatively sensitive to phenotype switching via α_1 and α_2, which together determine the number of chronic steady states that exist. For α_1 small or α_2 large, macrophage polarisation is driven primarily toward anti-inflammatory phenotypes and there exists a unique

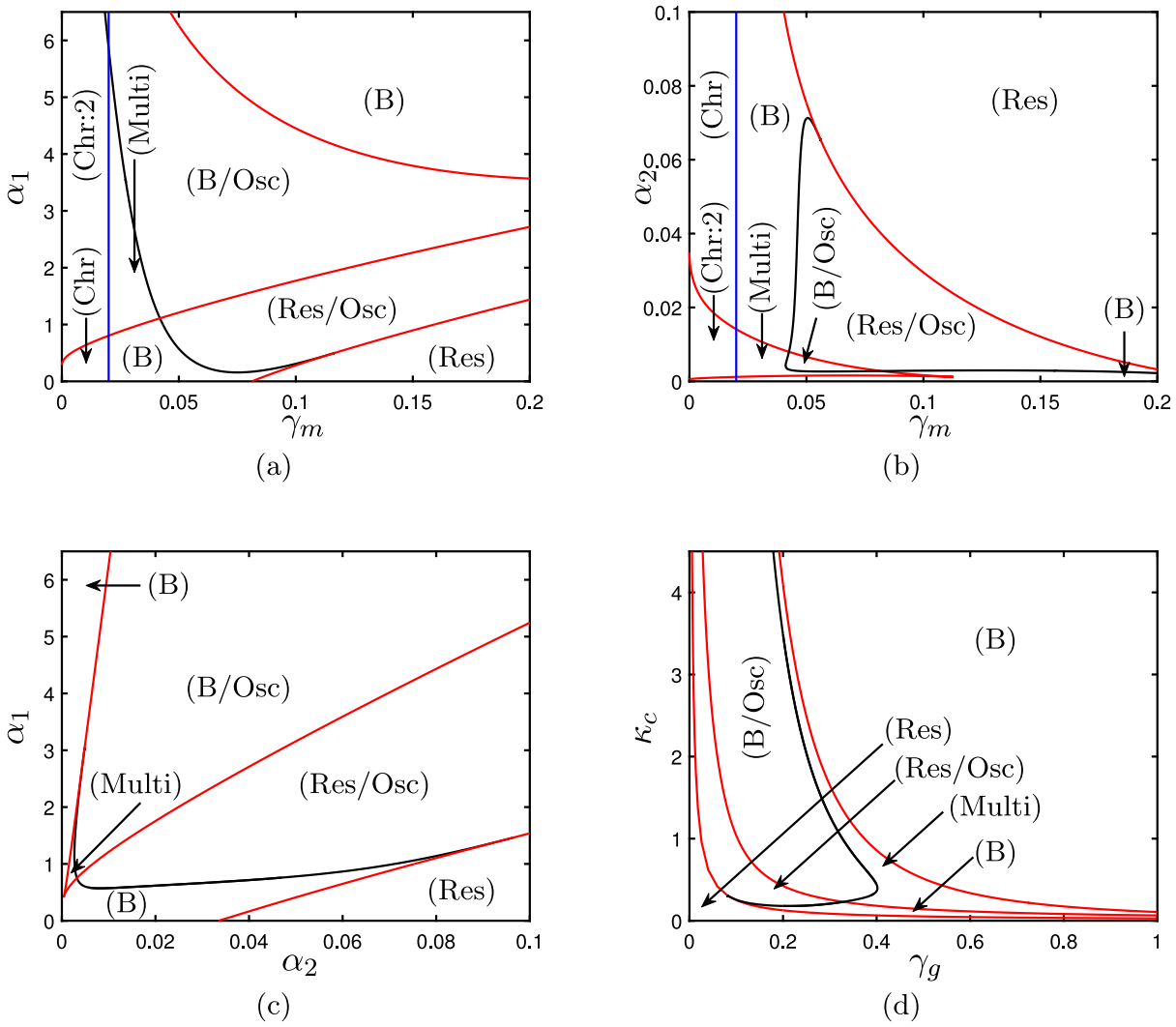

Fig. 4. Bifurcation diagrams illustrating bifurcations of (10)–(13) in two-dimensional slices of parameter space. Red curves represent saddle–node bifurcations; black curves represent Hopf bifurcations; blue curves represent transcritical bifurcations. All unspecified parameters are as given in Table 3. A list of abbreviations is given in Table 4.

chronic state corresponding to relatively low-level inflammation. For α_1 large or α_2 small, macrophage phenotype switching in the direction of pro-inflammatory phenotypes is stronger and we may obtain a second chronic steady state corresponding to more severe inflammation (*i.e.* with c larger). (See, also, Fig. 3(c,d).) For γ_m larger, so that the zero state is stable, α_1 and α_2 effect a switch in the existence/stability of chronic steady states, moving the model between configurations of guaranteed resolution (α_1 small or α_2 large) or bistability with both chronic and resolved outcomes permissible (α_1 large or α_2 small). This joint role of α_1 and α_2 is further elucidated in Fig. 4(c), in which we track bifurcations in (α_1, α_2)–space. For intermediate values of γ_m, α_1 and α_2, we find Hopf bifurcations that can give rise to oscillations as shown above in Figs. 2(b) and 3.

In Fig. 4(d), we draw similar conclusions regarding the parameters that control the concentrations of the two species of inflammatory mediators (*i.e.* κ_c, which controls the rate of growth of pro-inflammatory mediators, and γ_g, which controls the rate of decay of anti-inflammatory mediators population). Intuitively, for κ_c and γ_g both small, pro-inflammatory mediator concentrations are small and anti-inflammatory mediator concentrations are large, and the model attains a configuration in which resolution of inflammation is guaranteed. When these parameters are both large, chronic steady states are promoted and the model attains a bistable configuration (noting that the resolved state at zero is always stable here due to the values of γ_m and c_T satisfying (27)). Intermediate choices of κ_c and γ_g can give rise to oscillatory solutions or additional chronic states as we have already observed in Fig. 3(f,g).

3.3. Varying $R(p)$

We, here, investigate the extent to which our choice of recruitment function $R(p) = 1$ above influences the observed dynamics. That is, we seek to understand the manner in which the existence or stability of healthy and chronic outcomes depends upon the polarisation state of newly recruited macrophages. Here, we take $R(p)$ to be of a Gaussian-like shape given by

$$R(p) = \exp\left(-\frac{(p-\mu)^2}{\sigma^2}\right), \tag{29}$$

where μ parameterises the 'mean phenotype' of newly recruited macrophages and σ captures the level of variability in recruited macro phage phenotypes. In the limit $\mu \to 1$, newly recruited macrophages are primarily polarised toward pro-inflammatory activity, whereas the limit $\mu \to -1$ corresponds to recruitment of primarily anti-inflammatory phenotypes. We note that in the limit $\sigma \to \infty$ we have $R(p) \to 1$, and we recover the previous case of Section 3.2.

In Fig. 5, we show bifurcation diagrams akin to Fig. 3(a) but with $R(p)$ as given by (29), for a range of μ and σ values. Here, we treat

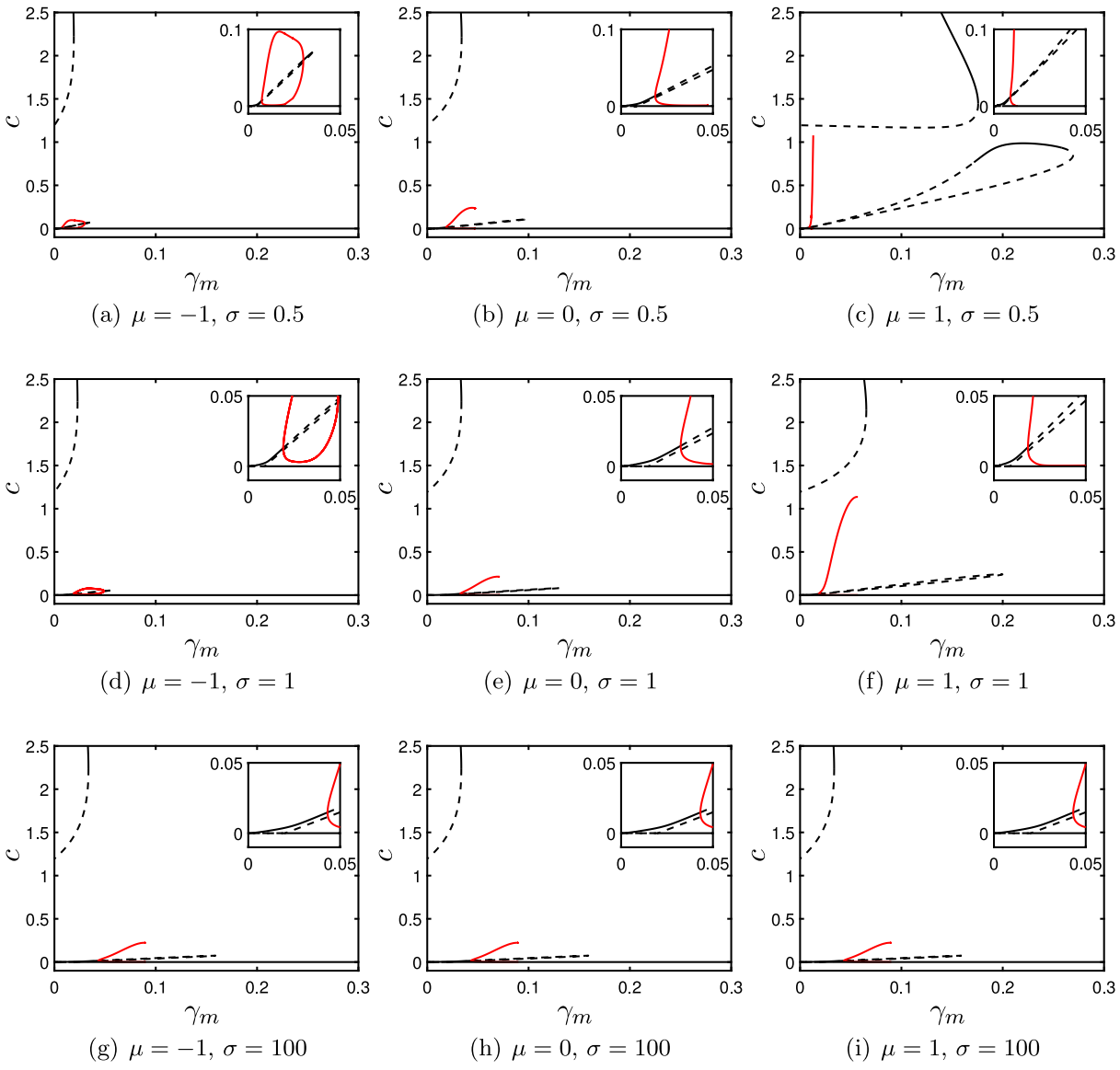

Fig. 5. Bifurcation diagrams illustrating solutions of (10)–(13) with $R(p)$ given by (29), for varying choices of μ and σ. All unspecified parameters are as in Table 3. Solid/dashed black curves represent stable/unstable steady state solutions. Solid red curves represent stable periodic orbits. (Unstable periodic orbits are omitted in (c) for clarity.).

the rate of macrophage loss γ_m as our primary bifurcation parameter and examine how the number and nature of steady states and the positions of related bifurcations are influenced by changes in $R(p)$. We note that, in principle, we could choose any of the seven parameters analysed in Fig. 3 as our bifurcation parameter here; however, our rationale for focusing upon γ_m in particular lies in the fact that this parameter (as a convenient proxy for the size of the macrophage population) has very direct biological interpretation, and has a well-understood role in affecting the stability of the zero-state via (27). In Fig. 3(a), for $R(p) = 1$, we observed that the healthy state is stable for $\gamma_m > 0.02$ (as per (27)), and for sufficiently large values of γ_m this is the only stable configuration. Additionally, two branches of chronic configurations exist for smaller choices of γ_m: a stable branch of low-level chronic solutions exists for $\gamma_m \lesssim 0.043$ and is then destabilised via a Hopf bifurcation giving rise to low-level oscillations supported by a primarily anti-inflammatory macrophage population; meanwhile, a second branch of higher-level chronic inflammation (supported by a largely pro-inflammatory macrophage population) exists for values of γ_m below a corresponding saddle–node bifurcation (at $\gamma_m \simeq 0.033$). As Fig. 5(g–i) show, we recover these results in the limit $\sigma \to \infty$. For $\sigma \sim \mathcal{O}(1)$, the three fundamental branches of solutions above persist, but may shift in parameter space and/or exhibit stability changes.

Taking the limit $\sigma \to 0$, so that the distribution of recruited macrophage phenotypes becomes increasingly narrow, results in some small changes to the location of the transcritical bifurcation that bounds the stability of the healthy steady state. However, this appears to be an artefact of having no normalising constant in (29) – a deliberate choice here to ensure that $R(p) \to 1$ as $\sigma \to \infty$. As we gradually reduce σ, we slightly slow the total rate of recruitment of new macrophages, and hence slightly enhance the stability of the healthy state (shifting the transcritical bifurcation to the left in Fig. 5). This behaviour is symmetrical in variations of μ.

Changes to the healthy steady state and its corresponding transcritical bifurcation are relatively slight in comparison to the influence of $R(p)$ upon chronic states. Intuitively, polarisation of recruited macrophages toward pro-inflammatory phenotypes has the effect of promoting chronic configurations. In the case of the higher-level chronic state of Fig. 3, the saddle node that provides the upper bound in γ_m for this branch shifts toward larger γ_m–values as $\mu \to 1$, rendering this state permissible for a broader range of choices of γ_m. Additionally, the limit $\mu \to 1$ can also drive stability changes on the low-level

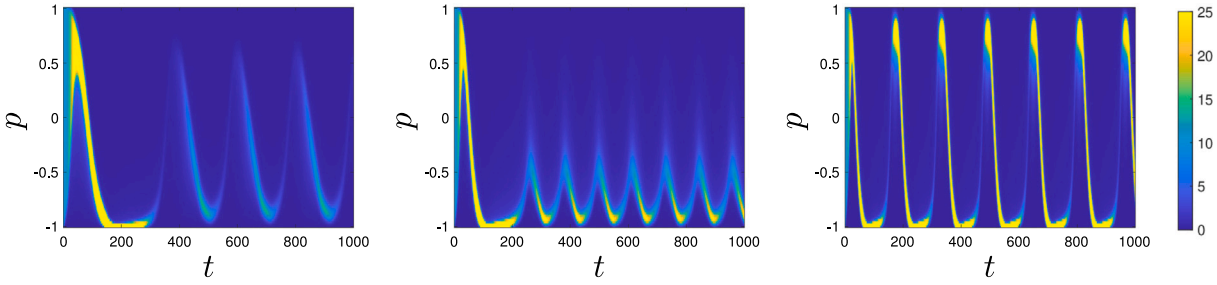

Fig. 6. Distributions of macrophage phenotypes, $m(t, p)$, for the oscillatory solutions of Fig. 5(d–f), for $\gamma_m = 0.035$ (and all unspecified parameters are as given in Table 3), for initial conditions $c(0) = g(0) = 0.5$ and $m(0, p) = 10$. The colour-bar represents the number density of each macrophage phenotype, with anti-inflammatory phenotypes at the base of the figures ($p = -1$) and pro-inflammatory phenotypes at the top of the figures ($p = 1$).

chronic branch, as shown for $\sigma = 0.5$ in Fig. 5(c). Here two additional (subcritical) Hopf bifurcations are introduced, providing additional stable steady-state solutions (and unstable periodic orbits, not plotted) in regions of parameter space in which restoration of the healthy state was previously guaranteed.

Interrogating the distributions of macrophage phenotypes that underlie the branches of solutions shown in Fig. 5 reveals that steady state solutions qualitatively recover the two steady state cases shown in Fig. 2 (a,c) regardless of our choice of $R(p)$. That is, chronic steady states involve strong polarisation of macrophages toward the pro-inflammatory end of the spectrum (similar to Fig. 2(a)), while resolution is generally preceded by polarisation of the macrophage population toward anti-inflammatory phenotypes (similar to Fig. 2(c)). However, oscillatory solutions do exhibit some dependence on the prescription of $R(p)$. In Fig. 6, we plot the temporal evolution of the distribution of macrophage phenotypes corresponding to the oscillations found at $\gamma_m = 0.035$ in Fig. 5(d–f). As observed for $R(p) = 1$ in Section 3.2, oscillatory solutions continue to require a reasonably significant number of anti-inflammatory macrophages. However, taking $\mu \to 1$, so that recruited macrophages are biased toward pro-inflammatory phenotypes, can intuitively result in oscillatory solutions that encompass a much broader range of phenotypes than previously observed. In particular, the oscillatory solution shown in Fig. 6(c) includes macrophages of phenotypes spanning the vast majority of the interval $p \in [-1, 1]$.

In Fig. 7, we track the γ_m–coordinates of the bifurcations shown in Fig. 5 as we vary σ, for $\mu = -1$ (dashed lines) and $\mu = 1$ (solid lines). At the top of the figure, as $\sigma \to \infty$, all bifurcation curves converge to the corresponding γ_m–coordinates of the bifurcations in Fig. 3(a). As we reduce σ, the extent to which the dashed and solid lines diverge from one-another reflects the extent to which the model is sensitive to the prescription of $R(p)$. Shown in blue in Fig. 7, the position of the transcritical bifurcation that determines the stability of the healthy zero state has very weak dependence on σ; furthermore, its position is identical for $\mu = -1$ and $\mu = 1$. The healthy state is unstable to the left of the illustrated blue curve, guaranteeing chronic outcomes here. As we move from $\mu = -1$ toward $\mu = 1$, the saddle–node bifurcation that bounds the high-level branch of chronic solutions (shown in magenta) traverses left to right, yielding an expanding region of stable, high-level chronic solutions as σ reduces. Meanwhile, for $\sigma \sim \mathcal{O}(1)$, the low-level chronic branch expands as $\mu \to 1$ or shrinks as $\mu \to -1$. As shown in Fig. 3(a), solutions on the low-level chronic branch are mostly unstable in the limit $\sigma \to \infty$; however, for $\mu \sim 1$, reducing σ ultimately results in a pair of new subcritical Hopf bifurcations which bound a region of additional stable steady states on this low-level branch. These additional stable states exist below the corresponding black curve in Fig. 7. These additional Hopf bifurcations collide with the corresponding saddle–node branch via fold–Hopf bifurcations at the points labelled "FH" in Fig. 7.

4. Discussion

Macrophages are highly plastic cells with the propensity to polarise into a diverse spectrum of phenotypes. Our model, presented here, has sought to address the fact that many previous mathematical models of inflammation-related systems take one of two approaches to describing diverse macrophage populations: either by incorporating a single homogenised population that averages phenotype-specific interactions; or, by incorporating two distinct and opposing phenotypes, typically representing *e.g.* the M1/M2 categorisation nomenclature. Instead, our model allows for intermediate phenotypes, by placing all possible macrophage phenotypes on a continuous spectrum according to their levels of pro/anti-inflammatory activity. Our model incorporates phenotype switching via nonlinear flux terms that are enhanced by environmental cues, with high concentrations of pro-inflammatory mediators driving macrophages to polarise toward pro-inflammatory phenotypes (synonymous with the M1 classification), and high concentrations of anti-inflammatory mediators driving the converse (resulting in phenotypes associated with tissue resident macrophages and the M2 classification). Through numerical simulation (in Matlab) and bifurcation analysis (in XPPAUT), we have examined the manner in which the rates of macrophage population growth, phenotype switching, and mediator interactions affect switches between healthy and chronic outcomes.

We note that macrophage numbers in tissues can increase due to both proliferation and recruitment, or a combination of both of these [47]. In our model, we do not distinguish between these mechanisms explicitly; however, we assume that the net effect of these mechanisms can be modelled via a corresponding logistic growth term (in (3)) up to a tissue-specific carrying capacity m^*_{max}. Importantly, our model incorporates, via the function $R(p)$, the potential for us to specify the phenotype-coordinates of macrophages that are newly added to the tissue of interest. For simplicity and mathematical tractability, we began our analysis by focusing on the case $R(p) = 1$ representing the idea that all phenotypes are recruited uniformly. While this is unlikely to be biologically realistic in many settings, this provided a useful starting point for our analysis, and allowed us to separately examine the manner in which variations in $R(p)$ affect the resulting dynamics.

For $R(p) = 1$, we observed that the model exhibits three fundamental types of solution, as follows. Firstly, the model may attain a steady state in which all components of the model reach zero. We regard this as a 'healthy' state, since it encompasses no inflammatory stimuli. This zero state is stable provided that the rate of macrophage loss (γ^*_m) sufficiently outweighs the basal rate of macrophage proliferation/recruitment in the absence of pro-inflammatory mediators (c^*_T), as per (27). Secondly, the model may attain a chronic steady state with positive numbers of macrophages and (in particular) pro-inflammatory mediators. Often, these chronic steady states are supported by a macrophage population that is mostly polarised toward

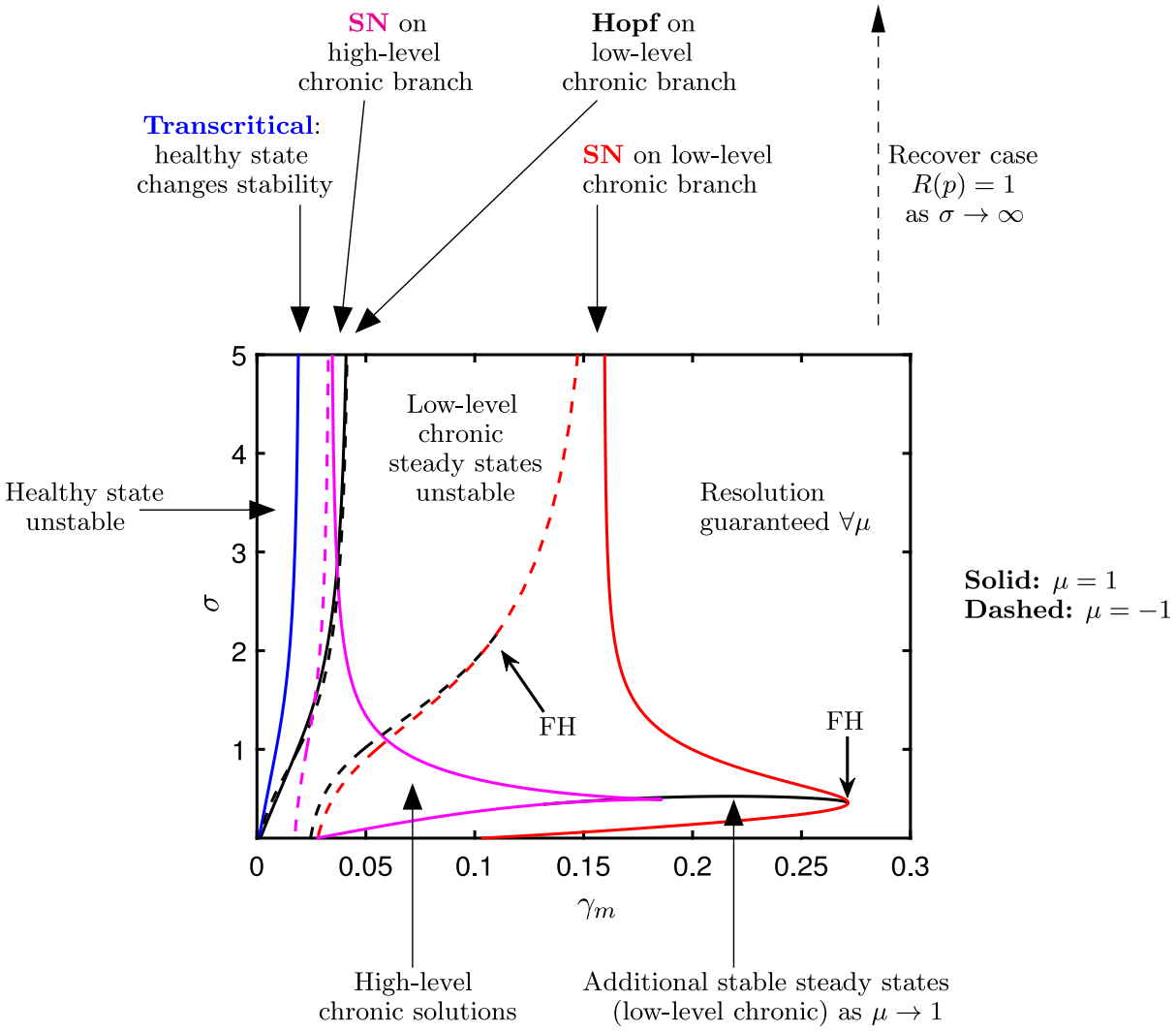

Fig. 7. Bifurcation diagram illustrating how the bifurcations of Fig. 3(a) move as we vary μ and σ in (29). As $\sigma \to \infty$, we recover the bifurcation coordinates of Fig. 3(a), for $R(p) = 1$. Solid and dashed curves illustrate the positions of bifurcations for $\mu = 1$ and $\mu = -1$ respectively. Red and magenta curves represent distinct sets of saddle–node bifurcations; black curves represent Hopf bifurcations. The blue curve represents the position of the transcritical bifurcation where the zero state changes stability, and is identical for $\mu = \pm 1$. FH = fold-Hopf bifurcation.

pro-inflammatory phenotypes. Thirdly, the model may converge toward stable oscillatory solutions that are reminiscent of conditions that exhibit relapsing-remitting characteristics. Throughout our analysis, oscillatory solutions have always been supported by macrophage populations that are mostly polarised toward anti-inflammatory phenotypes, with periods of remission generally corresponding to a macrophage population that almost entirely lies close to $p = -1$, and inflammatory flare-ups corresponding to surges in macrophages of more pro-inflammatory phenotypes (such as in Fig. 2(b)). (This has some similarity to conditions such as rheumatoid arthritis, whose oscillatory timecourses involve a complex dependence upon both M1 and M2 macrophages, as well as intermediate phenotypes [48].) In many areas of parameter space, two or more of the above solutions co-exist, and the model is bistable or multistable, with resulting inflammatory outcomes dependent upon our choice of initial conditions. In Figs. 3 and 4, we exposed the extent to which the existence/stability of the above solutions depends upon our model parameters. In particular, we observed that rapid rates of macrophage loss (γ_m^*) can eliminate chronic outcomes entirely (since macrophages are the only pro-inflammatory source in this model), while rapid macrophage proliferation/recruitment (c_T^*) promotes chronic outcomes, and that strong rates of macrophage phenotype switching toward pro-inflammatory phenotypes (α_1^*) promotes chronic steady-state outcomes, while phenotype switching toward anti-inflammatory phenotypes (α_2^*) can promote both resolution and low level chronic oscillations (in a manner that is dependent upon the model's remaining parameters).

In Section 3.3, we examined the extent to which the observations above are sensitive to our prescription of the phenotype of newly recruited macrophages. To do so, we set the corresponding recruitment function $R(p)$ to have a Gaussian-like shape, and examined the effects of variation of the mean (μ) and standard deviation (σ) of this Gaussian. In the limit $\sigma \to \infty$, our analysis recovers the case $R(p) = 1$ exactly. For $\sigma \sim \mathcal{O}(1)$, while the fundamental solutions discussed for $R(p) = 1$ above still persist, the locations of corresponding bifurcation points shift somewhat as a function of the recruited macrophage phenotype. Our analysis revealed that the stability of the healthy (zero) state exhibits very weak sensitivity to the phenotype of recruited macrophages, and instead depends more broadly on overall macrophage numbers. This is partially an artefact of the fact that our prescription of the pro-inflammatory mediator production function $f_2(p)$ in (7) equips all macrophages with $p \neq 1$ with at least some pro-inflammatory influence. Chronic solutions, however, exhibit more sensitivity to recruited phenotypes, with recruitment weighted toward pro-inflammatory phenotypes ($\mu \to 1$) resulting in the expansion of regions of parameter space that permit

chronic outcomes and (in some cases) the creation of new chronic steady state configurations. Meanwhile, biasing macrophage recruitment toward anti-inflammatory phenotypes ($\mu \to -1$) largely promotes resolution of inflammation. We highlight, once again, that the function $R(p)$ here incorporates both proliferation of existing macrophages and recruitment of new macrophages from the vasculature. This provides a potentially complex landscape of newly added macrophage phenotypes, with proliferation of existing tissue resident macrophages more likely to provide macrophages polarised toward anti-inflammatory activity, and recruitment of macrophages from the blood stream more likely to provide macrophages that are pro-inflammatory in nature. In most biologically relevant cases, we expect the latter of these mechanisms to dominate, with Fig. 7 illustrating that this can result in a relatively complex spectrum of chronic outcomes.

It is helpful to draw comparisons of our PDE model against previous ODE models of similar macrophage interactions in inflammatory settings. In particular, we note that our PDE model presented here is designed as a natural extension of "Model 2" of [32] to account for intermediate macrophage phenotypes. Broadly, we find that many of our observations share commonality with those of "Model 2" in [32]. The macro-scale roles of each parameter indicated in Fig. 3 largely align with those of the previous ODE model: large rates of macrophage loss (γ_m) drive the model toward a healthy zero state, while γ_m small yields chronic configurations; oscillatory solutions exist for reasonably large macrophage populations (m_{max} large); and strong macrophage polarisation toward pro-inflammatory phenotypes (α_1) drives chronic outcomes with the converse (α_2) generally driving resolution. While these overarching conclusions result readily from both the ODE and PDE constructions of the model, some intermediate bifurcations do differ slightly. For example, one key difference between these models is that the ODE model exhibits a healthy steady state with positive anti-inflammatory components (macrophages and mediators), while the PDE model exhibits just a unique healthy state at zero. In the ODE model, the zero state tends to change stability through collision with the positive healthy state at a transcritical bifurcation, whereas in the PDE model the zero state bifurcates to a solution in which macrophages are slightly biased toward pro-inflammatory phenotypes (*e.g.* yellow configurations in Fig. 3). This is an artefact, partly, of our choice of f_2, which is non-zero for all $p \neq -1$, rendering all macrophage phenotypes with $p \neq -1$ slightly pro-inflammatory. We note that it is common for models of inflammation to regard a steady state at zero to correspond to resolution [22,23,26,27,49–51] on the basis that the cell population being modelled represents the extent to which cell numbers in a given tissue are elevated above a certain healthy homeostatic baseline. Our PDE model is in line with this perspective; however, we note that a reformulation of the model in which a baseline population of entirely anti-inflammatory (tissue resident) macrophages sits at or below $p = -1$, for example, would be a simple task to allow the model to recover the potential for positive healthy steady states to exist. Furthermore, we note that our PDE model incorporates a more advanced description of macrophage proliferation/recruitment than the corresponding ODE model of [32] does, which focuses entirely on proliferation of existing macrophages and a resultant source of entirely anti-inflammatory macrophages. Through our analysis above, particularly that of Section 3.3, we have illustrated that this more-advanced description has the potential to generate a more diverse range of solutions than is afforded by the corresponding ODE model. Additionally, a key observation from the PDE model is that oscillatory solutions are generally supported by a macrophage population that is largely polarised toward anti-inflammatory phenotypes. We also observe oscillatory solutions in the corresponding ODE model (which incorporates two explicit and opposing phenotypes); however, our PDE model more readily exposes the extent to which intermediate phenotypes may play a supporting role.

Two key observations of this model are that macrophage recruitment that is strongly polarised toward pro-inflammatory phenotypes (synonymous with the M1 classification) can provide a broadening spectrum of chronic outcomes (Figs. 5 and 7, for $\mu \to 1$), and that amplification of macrophage phenotype switching toward anti-inflammatory phenotypes (*cf.* M2 macrophages) via α_2^* can promote restoration of health. These conclusions align with corresponding *in vitro* observations. For example, elevated numbers of M1 macrophages (versus M2) are linked to the onset of various inflammation-related conditions, including diabetes [52], osteoarthritis [53,54], and neurodegenerative conditions [55]. Moreover, actively manipulating macrophage phenotypes is an area of focus in the treatment of many conditions [33,34]. In rheumatoid arthritis, for example, various macromolecular interventions (as well as disease modifying anti-rheumatic drugs; DMARDs) have been identified (in animal tests) to both block M1 activation and stimulate polarisation toward the M2 phenotype. A thorough review of these is given by [56]. Furthermore, some treatments improve patient outcomes by explicitly depleting macrophage numbers, in order to downscale the pro-inflammatory feedbacks of (particularly M1) macrophages [34]. We observe corresponding features in our analysis of this model; for example, rapid rates of macrophage loss (γ_m large) generally result in the model reaching a monostable configuration in which a healthy outcome is guaranteed (see *e.g.* Figs. 3(a), 5 and 7).

In constructing our PDE model, we have modelled the complex range of macrophage phenotypes on a continuous spectrum of inflammatory activity. This has presented novel mathematical insight into the role of intermediate phenotypes, in particular. However, we note that the biological classification of specific macrophage phenotypes and where they may sit on our inflammatory spectrum is an extremely complex task that is hampered not only by the multi-factorial nature of macrophages' roles in inflammation, but also by a significant lack of experimental data against which to validate mathematical models of inflammation in general. In order to construct the model, we have deployed reasonably speculative choices of fluxes representing phenotype-switching ($\mathbf{q}^{+*}$, $\mathbf{q}^{-*}$) and terms representing the extent to which differing phenotypes produce differing levels of pro/anti-inflammatory mediators ($f_1(p)$ and $f_2(p)$, which we assume are linear in p here). Throughout, our approach has been to make the simplest possible choices of such terms, while retaining essential biological realism. However, we note that our choices of f_1 and f_2, in particular, are likely to somewhat over-simplify a more complex dependence upon phenotype. Our model elucidates the role that intermediate phenotypes can play in a complex inflammatory environment, but (as with any other mathematical model of inflammation) requires greater availability of experimental data in order to fully justify some inherent modelling assumptions. This remains an area for consideration in the future, should further experimental data become available. Additionally, a natural extension of the current model could be to additionally incorporate other immune cell populations (*e.g.* neutrophils, as studied in previous ODE models including [22] and "Model 3" of [32]). Given the anticipated complexity of the resultant models, we leave this is a target for future work.

In closing, we note that mathematical models of inflammatory systems such as that presented here have the propensity to identify the dominant mechanisms in driving the switch between chronic configurations and resolution of inflammatory damage, and hence exhibit scope to contribute to the identification of novel therapeutic targets. Being a key regulator of the inflammatory response, it is crucial that mathematical models adopt robust descriptions of relevant macrophage populations that include the possibility for intermediate phenotypes. With the scientific perspective on potential macrophage phenotypes continuing to rapidly evolve, there is great scope for continued development of mathematical models with more finessed descriptions of polarisation states that, with careful parameterisation, may ultimately contribute to the identification of new treatments.

CRediT authorship contribution statement

Suliman Almansour: Writing – review & editing, Writing – original draft, Visualization, Software, Investigation, Formal analysis, Data curation. **Joanne L. Dunster:** Writing – review & editing, Methodology, Conceptualization. **Jonathan J. Crofts:** Writing – review & editing, Supervision, Methodology. **Martin R. Nelson:** Writing – review & editing, Writing – original draft, Visualization, Supervision, Software, Project administration, Methodology, Investigation, Conceptualization.

Declaration of competing interest

The authors have no conflict of interest to declare.

Data availability

A repository of supporting codes is available; a link is provided in the manuscript.

Acknowledgment

JLD is gratefully supported by the British Heart Foundation (RG/20/7/34866).

Appendix. Numerical scheme

We solve the system (10)–(13) numerically via a method of lines approach, by discretising in the phenotype variable, p, to obtain a system of ODEs which we solve via in-built ODE solvers in Matlab and XPPAUT.

We discretise in p by introducing $N+1$ equally-spaced meshpoints p_j given by

$$p_j = -1 + j\,\mathrm{d}p \qquad \text{for } j = 0, \dots, N, \tag{A.1}$$

where $\mathrm{d}p = 2/N$ is the corresponding meshpoint spacing. Furthermore, we write $m_j(t) \simeq m(t, p_j)$ to represent the approximation of the macrophage variable at a given phenotype meshpoint.

We approximate the flux terms in (10) via standard, first-order finite difference approximations. To ensure numerical stability, we take an upwinding approach in which we choose forward or backward finite difference approximations depending on the direction of the flux. Since the term containing $\alpha_1 c$ represents flux in the positive p–direction, we employ a backward difference approximation for the derivative evaluated on meshpoint j, writing

$$\frac{\partial}{\partial p}\left((1-p)\,m\right)\Big|_{p=p_j} = \frac{1}{\mathrm{d}p}\left(\left(1-p_j\right)m_j - \left(1-p_{j-1}\right)m_{j-1}\right) + \mathcal{O}(\mathrm{d}p), \tag{A.2}$$

for all $j = 1, \dots, N$. Conversely, since the term containing $\alpha_2 g$ represents flux in the negative p–direction, we employ the following forward difference approximation:

$$\frac{\partial}{\partial p}\left((1+p)\,m\right)\Big|_{p=p_j} = \frac{1}{\mathrm{d}p}\left(\left(1+p_{j+1}\right)m_{j+1} - \left(1+p_j\right)m_j\right) + \mathcal{O}(\mathrm{d}p), \tag{A.3}$$

for all $j = 0, \dots, N-1$. On the boundaries, we adapt (A.2) and (A.3) to reflect that $m = 0$ for all points outside of the domain $p \in [-1, 1]$, writing

$$\frac{\partial}{\partial p}\left((1-p)\,m\right)\Big|_{p=p_0} = \frac{1}{\mathrm{d}p}\left(1-p_0\right)m_0 + \mathcal{O}(\mathrm{d}p), \tag{A.4}$$

$$\frac{\partial}{\partial p}\left((1+p)\,m\right)\Big|_{p=p_N} = -\frac{1}{\mathrm{d}p}\left(1+p_N\right)m_N + \mathcal{O}(\mathrm{d}p). \tag{A.5}$$

We evaluate the integrals in (11) and (12) via trapezium rule, writing

$$\int_{-1}^{1} f_i(p)m\,\mathrm{d}p \simeq \frac{dp}{2}\left(f_i\left(p_0\right)m_0 + f_i\left(p_N\right)m_N + 2\sum_{j=1}^{N-1} f_i\left(p_j\right)m_j\right) \equiv F_i(t), \tag{A.6}$$

for $i = 1, 2$. Similarly, we evaluate $m_T(t)$ according to

$$m_T(t) \simeq \frac{dp}{2}\left(m_0 + m_N + 2\sum_{j=1}^{N-1} m_j\right). \tag{A.7}$$

Under these approximations, the system (10)–(13) gives rise to the following system of $N+3$ ODEs at leading order:

$$\begin{aligned}\frac{\mathrm{d}m_0}{\mathrm{d}t} &= -\frac{\alpha_1 c}{\mathrm{d}p}\left(\left(1-p_0\right)m_0\right) + \frac{\alpha_2 g}{\mathrm{d}p}\left(\left(1+p_1\right)m_1 - \left(1+p_0\right)m_0\right)\\ &\quad + \left(c+c_T\right)R(p_0)m_T\left(1-\frac{m_T}{m_{max}}\right) - \gamma_m m_0,\end{aligned} \tag{A.8}$$

$$\begin{aligned}\frac{\mathrm{d}m_j}{\mathrm{d}t} &= -\frac{\alpha_1 c}{\mathrm{d}p}\left(\left(1-p_j\right)m_j - \left(1-p_{j-1}\right)m_{j-1}\right)\\ &\quad + \frac{\alpha_2 g}{\mathrm{d}p}\left(\left(1+p_{j+1}\right)m_{j+1} - \left(1+p_j\right)m_j\right)\\ &\quad + \left(c+c_T\right)R(p_j)m_T\left(1-\frac{m_T}{m_{max}}\right)\\ &\quad - \gamma_m m_j, \qquad \text{for } j = 1, \dots, N-1,\end{aligned} \tag{A.9}$$

$$\begin{aligned}\frac{\mathrm{d}m_N}{\mathrm{d}t} &= -\frac{\alpha_1 c}{\mathrm{d}p}\left(\left(1-p_N\right)m_N - \left(1-p_{N-1}\right)m_{N-1}\right) + \frac{\alpha_2 g}{\mathrm{d}p}\left(-\left(1+p_N\right)m_N\right)\\ &\quad + \left(c+c_T\right)R(p_N)m_T\left(1-\frac{m_T}{m_{max}}\right) - \gamma_m m_N,\end{aligned} \tag{A.10}$$

$$\frac{\mathrm{d}g}{\mathrm{d}t} = F_1(t) - \gamma_g g, \tag{A.11}$$

$$\frac{\mathrm{d}c}{\mathrm{d}t} = \kappa_c F_2(t) - cg - c, \tag{A.12}$$

with $F_1(t)$, $F_2(t)$ and $m_T(t)$ as given in (A.6) and (A.7). Throughout this paper, numerical simulations and bifurcation analyses are based upon implementations of the system (A.8)–(A.12) in Matlab and XPPAUT with $N = 100$. In Matlab, this ODE system is solved using the in-built solver `ode45`. In XPPAUT, we implement the adaptive, implicit solver `CVODE` as described in [38]. We also note that implementation of the ODEs that result from semi-discretisation of a PDE system (such as (A.8)–(A.10)) is most easily achieved via the use of XPPAUT array structures; a useful tutorial that describes implementation of such systems is provided by [39]. In both Matlab and XPPAUT, convergence tests have been performed to ensure that our choice of N does not adversely affect the accuracy of our results; details are omitted here for brevity. Both Matlab and XPPAUT codes are available online at github.com/martinrnelson/MacrophageContinuum.

References

[1] D.L. Laskin, V.R. Sunil, C.R. Gardner, J.D. Laskin, Macrophages and tissue injury: agents of defense or destruction? Annu. Rev. Pharmacol. Toxicol. 51 (2011) 267–288.

[2] P.J. Murray, Macrophage polarization, Annu. Rev. Physiol. 79 (2017) 541–566.

[3] T.A. Wynn, A. Chawla, J.W. Pollard, Macrophage biology in development, homeostasis and disease, Nature 496 (7446) (2013) 445–455.

[4] P.J. Murray, T.A. Wynn, Protective and pathogenic functions of macrophage subsets, Nat. Rev. Immunol. 11 (11) (2011) 723–737.

[5] D.Y. Vogel, J.E. Glim, A.W. Stavenuiter, M. Breur, P. Heijnen, S. Amor, C.D. Dijkstra, R.H. Beelen, Human macrophage polarization in vitro: maturation and activation methods compared, Immunobiology 219 (9) (2014) 695–703.

[6] F.O. Martinez, S. Gordon, The M1 and M2 paradigm of macrophage activation: time for reassessment, F1000prime Rep. 6 (2014).

[7] P.J. Murray, J.E. Allen, S.K. Biswas, E.A. Fisher, D.W. Gilroy, S. Goerdt, S. Gordon, J.A. Hamilton, L.B. Ivashkiv, T. Lawrence, et al., Macrophage activation and polarization: nomenclature and experimental guidelines, Immunity 41 (1) (2014) 14–20.

[8] C. Yunna, H. Mengru, W. Lei, C. Weidong, Macrophage M1/M2 polarization, Eur. J. Pharmacol. 877 (2020) 173090.

[9] K.E. Martin, A.J. García, Macrophage phenotypes in tissue repair and the foreign body response: Implications for biomaterial-based regenerative medicine strategies, Acta Biomater. 133 (2021) 4–16.

[10] M. Cutolo, R. Campitiello, E. Gotelli, S. Soldano, The role of M1/M2 macrophage polarization in rheumatoid arthritis synovitis, Front. Immunol. 13 (2022) 867260.

[11] S. Reinartz, T. Schumann, F. Finkernagel, A. Wortmann, J.M. Jansen, W. Meissner, M. Krause, A.-M. Schwörer, U. Wagner, S. Müller-Brüsselbach, et al., Mixed-polarization phenotype of ascites-associated macrophages in human ovarian carcinoma: correlation of CD163 expression, cytokine levels and early relapse, Int. J. Cancer 134 (1) (2014) 32–42.
[12] T.D. Smith, M.J. Tse, E.L. Read, W.F. Liu, Regulation of macrophage polarization and plasticity by complex activation signals, Integr. Biol. 8 (9) (2016) 946–955.
[13] G.T. Bardi, M.A. Smith, J.L. Hood, Melanoma exosomes promote mixed M1 and M2 macrophage polarization, Cytokine 105 (2018) 63–72.
[14] P. Calle, G. Hotter, Macrophage phenotype and fibrosis in diabetic nephropathy, Int. J. Mol. Sci. 21 (8) (2020) 2806.
[15] M.R. Owen, J.A. Sherratt, Mathematical modelling of macrophage dynamics in tumours, Math. Models Methods Appl. Sci. 9 (04) (1999) 513–539.
[16] H. Knútsdóttir, E. Pálsson, L. Edelstein-Keshet, Mathematical model of macrophage-facilitated breast cancer cells invasion, J. Theoret. Biol. 357 (2014) 184–199.
[17] T. Lelekov-Boissard, G. Chapuisat, J.-P. Boissel, E. Grenier, M.-A. Dronne, Exploration of beneficial and deleterious effects of inflammation in stroke: dynamics of inflammation cells, Phil. Trans. R. Soc. A 367 (1908) (2009) 4699–4716.
[18] I.U. Ahmed, H.M. Byrne, M.R. Myerscough, Macrophage anti-inflammatory behaviour in a multiphase model of atherosclerotic plaque development, Bull. Math. Biol. 85 (5) (2023) 37.
[19] M.C. Herald, General model of inflammation, Bull. Math. Biol. 72 (4) (2010) 765.
[20] K. Penner, B. Ermentrout, D. Swigon, Pattern formation in a model of acute inflammation, SIAM J. Appl. Dyn. Syst. 11 (2) (2012) 629–660.
[21] E.O. Bangsgaard, P.G. Hjorth, M.S. Olufsen, J. Mehlsen, J.T. Ottesen, Integrated inflammatory stress (itis) model, Bull. Math. Biol. 79 (2017) 1487–1509.
[22] J.L. Dunster, H.M. Byrne, J.R. King, The resolution of inflammation: a mathematical model of neutrophil and macrophage interactions, Bull. Math. Biol. 76 (2014) 1953–1980.
[23] A. Bayani, J.L. Dunster, J.J. Crofts, M.R. Nelson, Mechanisms and points of control in the spread of inflammation: a mathematical investigation, Bull. Math. Biol. 82 (4) (2020) 1–22.
[24] A. Bayani, J.L. Dunster, J.J. Crofts, M.R. Nelson, Spatial considerations in the resolution of inflammation: Elucidating leukocyte interactions via an experimentally-calibrated agent-based model, PLoS Comput. Biol. 16 (11) (2020) e1008413.
[25] K. Wendelsdorf, J. Bassaganya-Riera, R. Hontecillas, S. Eubank, Model of colonic inflammation: immune modulatory mechanisms in inflammatory bowel disease, J. Theoret. Biol. 264 (4) (2010) 1225–1239.
[26] J.L. Dunster, J.M. Gibbins, M.R. Nelson, Exploring the constituent mechanisms of hepatitis: a dynamical systems approach, Math. Med. Biol.: J. IMA 40 (1) (2023) 24–48.
[27] M.R. Nelson, J.M. Gibbins, J.L. Dunster, Platelet-driven routes to chaos in a model of hepatitis, Chaos Solitons Fractals 170 (2023) 113338.
[28] J. Lee, F.R. Adler, P.S. Kim, A mathematical model for the macrophage response to respiratory viral infection in normal and asthmatic conditions, Bull. Math. Biol. 79 (9) (2017) 1979–1998.
[29] R. Eftimie, C. Barelle, Mathematical investigation of innate immune responses to lung cancer: The role of macrophages with mixed phenotypes, J. Theoret. Biol. 524 (2021) 110739.
[30] L. Bartha, R. Eftimie, Mathematical investigation into the role of macrophage heterogeneity on the temporal and spatio-temporal dynamics of non-small cell lung cancers, J. Theoret. Biol. 549 (2022) 111207.
[31] S. Suveges, R. Eftimie, D. Trucu, Re-polarisation of macrophages within collective tumour cell migration: a multiscale moving boundary approach, Front. Appl. Math. Stat. 7 (2022) 799650.
[32] S. Almansour, J. Dunster, J. Crofts, M. Nelson, A systematic evaluation of the influence of macrophage phenotype descriptions on inflammatory dynamics, Math. Med. Biol. (2024) dqae004.
[33] K.L. Spiller, T.J. Koh, Macrophage-based therapeutic strategies in regenerative medicine, Adv. Drug Deliv. Rev. 122 (2017) 74–83.
[34] M. Ponzoni, F. Pastorino, D. Di Paolo, P. Perri, C. Brignole, Targeting macrophages as a potential therapeutic intervention: impact on inflammatory diseases and cancer, Int. J. Mol. Sci. 19 (7) (2018) 1953.
[35] R. Eftimie, Investigation into the role of macrophages heterogeneity on solid tumour aggregations, Math. Biosci. 322 (2020) 108325.
[36] A. El-Kenawi, C. Gatenbee, M. Robertson-Tessi, R. Bravo, J. Dhillon, Y. Balagurunathan, A. Berglund, N. Vishvakarma, A. Ibrahim-Hashim, J. Choi, et al., Acidity promotes tumour progression by altering macrophage phenotype in prostate cancer, Br. J. Cancer 121 (7) (2019) 556–566.
[37] J.A. Bull, H.M. Byrne, Quantification of spatial and phenotypic heterogeneity in an agent-based model of tumour-macrophage interactions, PLoS Comput. Biol. 19 (3) (2023) e1010994.
[38] B. Ermentrout, Simulating, Analyzing, and Animating Dynamical Systems: A Guide to XPPAUT for Researchers and Students, SIAM, Philadelphia, 2002.
[39] D.L. Gandy, M.R. Nelson, Analyzing pattern formation in the gray–scott model: an XPPAUT tutorial, SIAM Rev. 64 (3) (2022) 728–747.
[40] L.C. Davies, S.J. Jenkins, J.E. Allen, P.R. Taylor, Tissue-resident macrophages, Nat. Immunol. 14 (10) (2013) 986–995.
[41] C. Liu, D. Chu, K. Kalantar-Zadeh, J. George, H.A. Young, G. Liu, Cytokines: from clinical significance to quantification, Adv. Sci. 8 (15) (2021) 2004433.
[42] H.V. Waugh, J.A. Sherratt, Modeling the effects of treating diabetic wounds with engineered skin substitutes, Wound Repair Regen. 15 (4) (2007) 556–565.
[43] R.L. Cooper, R.A. Segal, R.F. Diegelmann, A.M. Reynolds, Modeling the effects of systemic mediators on the inflammatory phase of wound healing, J. Theoret. Biol. 367 (2015) 86–99.
[44] S.J. Jenkins, J.E. Allen, The expanding world of tissue-resident macrophages, Eur. J. Immunol. 51 (8) (2021) 1882–1896.
[45] W. Zhu, J. Yu, Y. Nie, X. Shi, Y. Liu, F. Li, X.-l. Zhang, Disequilibrium of M1 and M2 macrophages correlates with the development of experimental inflammatory bowel diseases, Immunol. Invest. 43 (7) (2014) 638–652.
[46] D. Lissner, M. Schumann, A. Batra, L.-I. Kredel, A.A. Kühl, U. Erben, C. May, J.-D. Schulzke, B. Siegmund, Monocyte and M1 macrophage-induced barrier defect contributes to chronic intestinal inflammation in IBD, Inflamm. Bowel Dis. 21 (6) (2015) 1297–1305.
[47] D. Rückerl, J.E. Allen, Macrophage proliferation, provenance, and plasticity in macroparasite infection, Immunol. Rev. 262 (1) (2014) 113–133.
[48] M. Cutolo, R. Campitiello, E. Gotelli, S. Soldano, The role of M1/M2 macrophage polarization in rheumatoid arthritis synovitis, Front. Immunol. 13 (2022) 867260.
[49] A. Reynolds, J. Rubin, G. Clermont, J. Day, Y. Vodovotz, G.B. Ermentrout, A reduced mathematical model of the acute inflammatory response: I. Derivation of model and analysis of anti-inflammation, J. Theoret. Biol. 242 (1) (2006) 220–236.
[50] C. Bianca, L. Guerrini, J. Riposo, A delayed mathematical model for the acute inflammatory response to infection, Appl. Math. Inf. Sci. 9 (6) (2015) 2775.
[51] L. Caudill, F. Lynch, A mathematical model of the inflammatory response to pathogen challenge, Bull. Math. Biol. 80 (2018) 2242–2271.
[52] I. Torres-Castro, Ú.D. Arroyo-Camarena, C.P. Martínez-Reyes, A.Y. Gómez-Arauz, Y. Dueñas-Andrade, J. Hernández-Ruiz, Y.L. Béjar, V. Zaga-Clavellina, J. Morales-Montor, L.I. Terrazas, et al., Human monocytes and macrophages undergo M1-type inflammatory polarization in response to high levels of glucose, Immunol. Lett. 176 (2016) 81–89.
[53] B. Liu, M. Zhang, J. Zhao, M. Zheng, H. Yang, Imbalance of M1/M2 macrophages is linked to severity level of knee osteoarthritis, Exp. Ther. Med. 16 (6) (2018) 5009–5014.
[54] A. Ummarino, F.M. Gambaro, E. Kon, F. Torres Andón, Therapeutic manipulation of macrophages using nanotechnological approaches for the treatment of osteoarthritis, Nanomaterials 10 (8) (2020) 1562.
[55] Y. Tang, W. Le, Differential roles of M1 and M2 microglia in neurodegenerative diseases, Mol. Neurobiol. 53 (2016) 1181–1194.
[56] S. Tardito, G. Martinelli, S. Soldano, S. Paolino, G. Pacini, M. Patane, E. Alessandri, V. Smith, M. Cutolo, Macrophage M1/M2 polarization and rheumatoid arthritis: a systematic review, Autoimmun. Rev. 18 (11) (2019) 102397.